Sato, Keisuke; Toda, Yuji; Tsujimoto, Tetsuro

Modelling of River Flow and Sediment Load Based on the Hydrological Behavior Model in Yahagi River Basin, Japan

MODELLING OF RIVER FLOW AND SEDIMENT LOAD BASED ON THE HYDROLOGICAL BEHAVIOR MODEL IN YAHAGI RIVER BASIN, JAPAN

Keisuke Sato[1], Yuji Toda[2] and Tetsuro Tsujimoto[3]

[1] Researcher, Department of Civil Engineering, Nagoya University, Japan
Furocho, Chikusa-Ku, Nagoya, 464-8603, Japan, e-mail: sato@civil.nagoya-u.ac.jp
[2] Associate Professor, Department of Civil Engineering, Nagoya University, Japan
Furocho, Chikusa-Ku, Nagoya, 464-8603, Japan, e-mail: ytoda@cc.nagoya-u.ac.jp
[3] Professor, Department of Civil Engineering, Nagoya University, Japan
Furocho, Chikusa-Ku, Nagoya, 464-8603, Japan, e-mail: ttsujimoto@genv.nagoya-u.ac.jp

ABSTRACT

Ecosystem services in the river region should be assessed by the condition of flow rate, water stage, bed morphology/materials and water quality. In addition to natural phenomena, anthropogenic influences such as river water withdrawal/discharge are not negligible for assessment in real river watersheds. With these considerations, the objectives of this research are to design of simple procedure to estimate flow rate and sediment load by using existing hydrological behavior model and to apply the modelling method to the Yahagi River Basin, which is a part of Ise Bay Basin located in the central region of Japan.

Natural river networks and sub-basins were separated with anastomosis points automatically. Additionally, effects of artificial water transportation and sediment accumulation into the dams were considered. Each sub-basin was divided into six landuse, which were the minimum spatial unit used in runoff calculation.

As a result, a semi-automated procedure of the watershed modelling was used to assess the river flow and the sediment load. Through application to the Yahagi River Basin, outflow time series in the pervious land were calculated showing recognizable differences depending on the runoff process. Although comparatively high correlations (R^2>0.65) between calculated flow and observed flow in every river segment were shown, a part of the flood flow in the middle- and down-stream was underestimated. These disagreements may be caused by the incorrect estimation of surface runoff rate in land other than forest. Also, calculated sediment load in normal flow conditions was overestimate because reproducibility of suspended load from river bed storage was inadequate, whereas calculated L-Q relations were identical with those of observation over a range of high sediment load (high river flow).

Keywords: hydrological behavior model (BASINS4.0 and HSPF12.0), runoff processes, landuse, hourly river flow, sediment load and GIS

1. Introductions

Estimation of ecosystem services (Robert *et al*., 1997) is an extremely effective method for the eco-compatible and sustainable watershed management. It should be understood that ecosystem services have to be evaluated for various type of services in each characteristic region categorized as habitat environment which in turn is described by using physical properties (Tsujimoto *et al*., 2008). Especially, ecosystem services in the river region should be assessed by the condition of flow rate, water stage, bed morphology/materials and water quality. Because the type and ability of service varies a great deal depending on the conditions

above, it is necessary to estimate temporal-spatial distribution of the river conditions by observation and modelling. Additionally, anthropogenic influences such as landuse change and river water withdrawal/discharge (Hanasaki *et al.*, 2005) are not negligible for the assessment in real river watersheds (Nawarathna *et al.*, 2002; Tebakari *et al.*, 2002; Wongsa and Shimizu, 2003; Toda *et al.*, 2006).

With these considerations and background, we have suggested a new eco-compatible environmental assessment method for watershed regions based on soundness of their ecosystem services. The framework of the assessment (Tsujimoto *et al.*, 2008) in the research project, "Research and Development in Assessment and Restoration for Eco-compatible Management of River Basin Complex around Ise Bay" promoted by the Japan Special Coordination Fund for Promoting Science and Technology for Sustainable National Land Management, is expressed in figure 1. Two main frames which were "flux network modelling" and "mechanism for elucidation of ecosystem" were quantitatively integrated together to assess the services. This research especially focuses on the "flux network modelling". Then, specific objectives are set to design a simple procedure to estimate flow rate and sediment load by using an existing hydrological behavior model (BASINS Ver.4.0 and HSPF Ver.12, U.S.EPA, http://www.epa.gov/waterscience/basins), and to apply the modelling method to the Yahagi River Basin, which is a part of the Ise bay basin located in the central region of Japan.

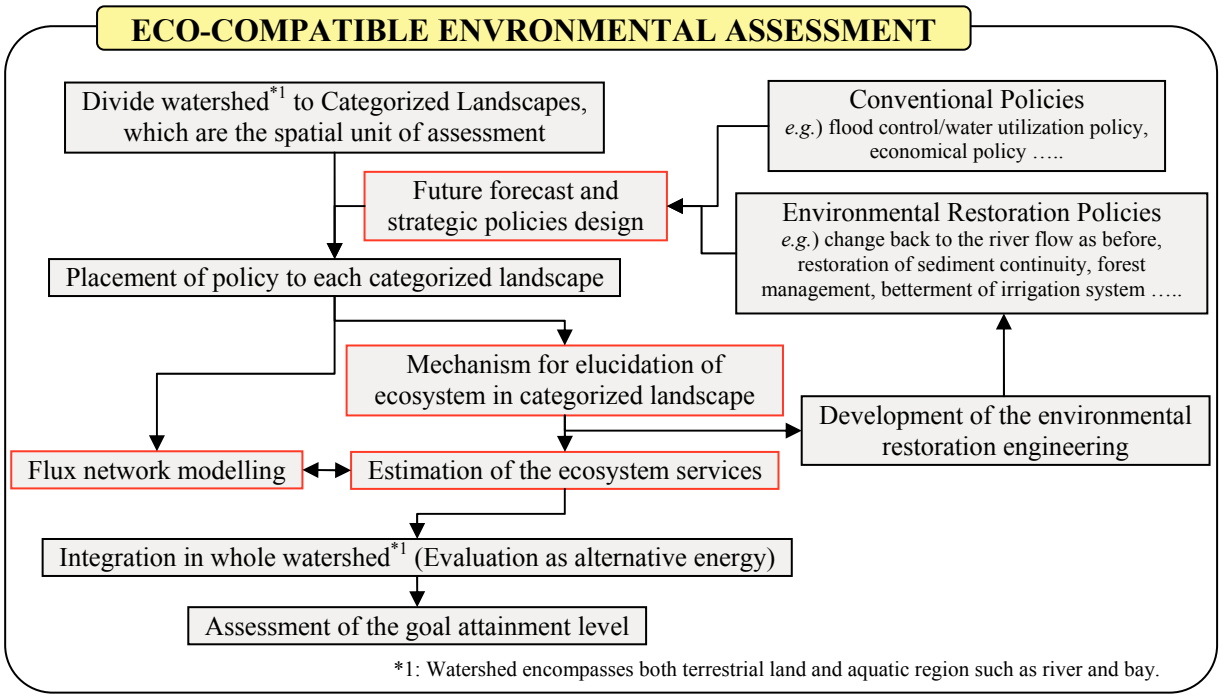

Figure 1: framework and procedure of eco-compatible environmental assessment for the watershed region based on soundness of the ecosystem services (Tsujimoto *et al.*, 2008).

2. Materials and Methods

Characteristics of the Target Basin (Yahagi River Basin)

Location of the Yahagi River Basin encompassing Yahagi Old River Basin (1,904km^2) is shown in figure 2. The main stream (Yahagi River, 118km) originates from the Central Japanese Alps (Kiso Mountains, 1,908m) and is separated into two channels (a

previous main river and a flood way) at 14 km point from the river mouth, and eventually flows into Mikawa Bay (a part of Ise bay). The longitudinal shape/gradient of the Yahagi River are displayed in figure 3. Its averaged slope is approx. 1/80 (similar to other Japanese rivers). In this research, the target basin was set to the Yahagi River Basin excluding the tidal river compartment and its watershed. Therefore, an outlet point of the Yahagi River Basin (1,740km^2) was set at the 10.6 km point (Yonedzu automatic observing station) from the river mouth.

This region belongs to monsoonal climate with annual precipitation in the Yahagi River Basin approx. 1,670mm (averaged in past ten years, 1993-2002). There are one multi-purpose dam (Yahagi Dam), one agricultural dam (Habu Dam), four hydroelectric dams (>10,000kW) and three head works (Meiji, Hosokawa and Otogawa) in the river basin; however many small weirs have been constructed in the basin. Historical trends of precipitation upstream, river flow volume at the Meiji head works, without any water withdrawals, and ratio of the total water withdrawal to river flow volume are shown in figure 4. It was found that annual precipitation and river flow are significantly (twice) different although total water withdrawal varies only slightly as approx. 500mm/year (except hydroelectric water). Therefore, ratios of total water withdrawal to river flow without any water withdrawal (*i.e.*, water resource) differed considerably from year to year (30-60%). By focussing on constituents of water withdrawal, the agricultural water makes up more than half of total water withdrawal (56% in average). This agricultural water has been provided to agricultural land including paddy fields (15,161ha, Aichi pref.) located both inside and outside Yahagi River Basin.

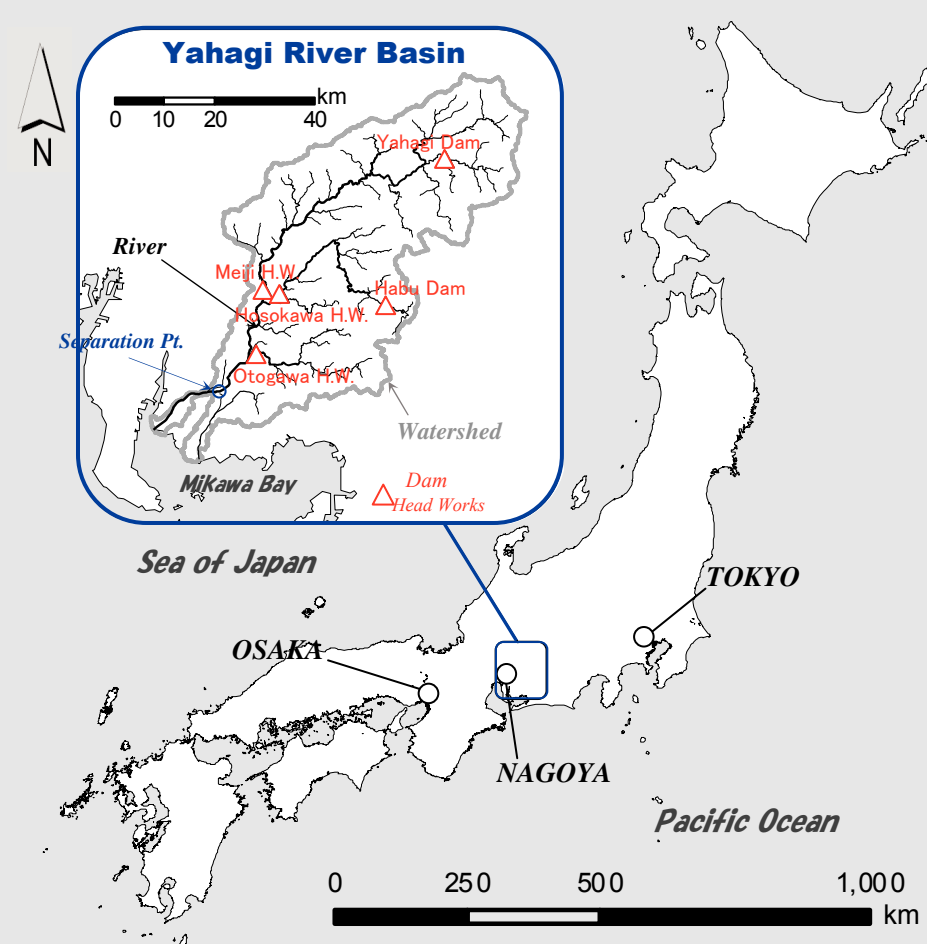

Figure 2: Location of Yahagi river network, its basin, and dams (head works).

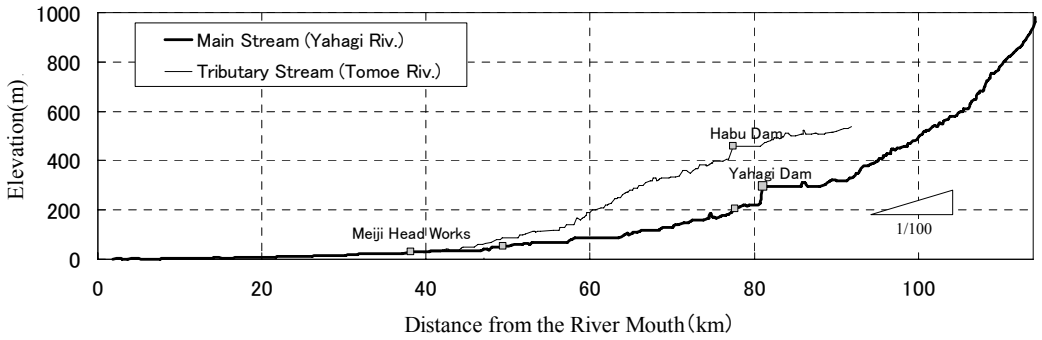

Figure 3: Longitudinal shapes estimated by the Digital Elevation Model (Digital Map 50m, Geographical Survey Institute, Japan) and GIS tools (Special Tools of Hydrology Modelling and ET Geowizards Ver.9.8 on ESRI ArcGIS Ver.9.2).

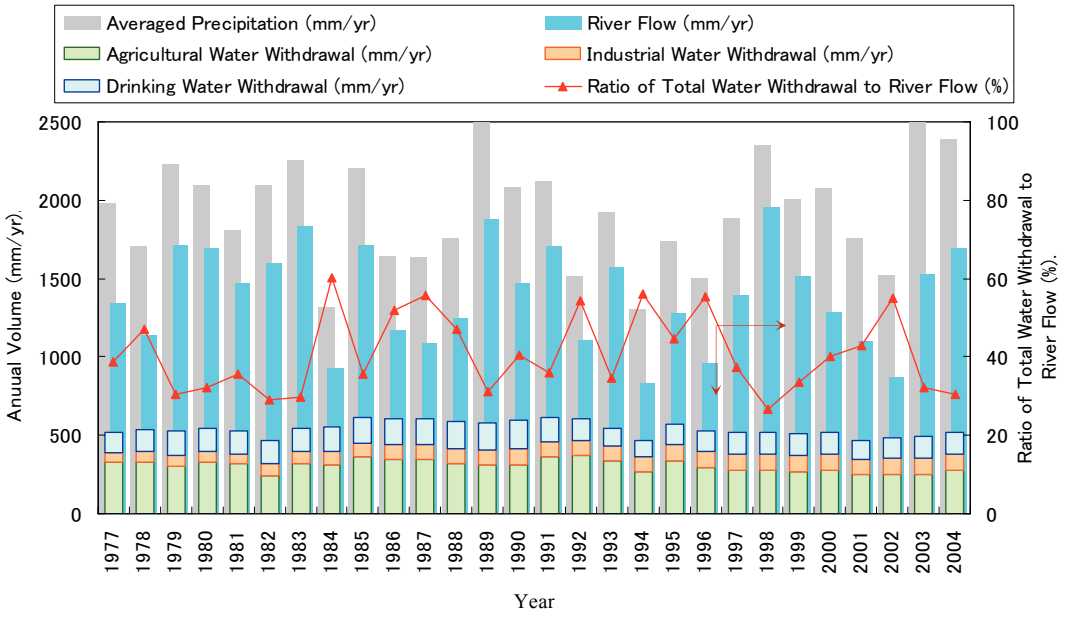

*Precipitation was weighted mean value in five observing station (Hiraya, Kamiyahagi, Neba, Nagura and Yahagi dam) located in upstream.
*River flow was the volume at Meiji head works, including any water withdrawal in upstream.
*Water withdrawal was the total volume in whole basin for each utilization purpose except hydroelectric water.
*Data source: Agriculture, Forestry and Fisheries office of Nishimikawa region, Aichi Prefecture (2004).

Figure 4: Historical trends of precipitation in upstream, river flow volume at the Meiji head works, without any water withdrawals, and ratio of total water withdrawal to river flow volume.

Modelling Methodology

BASINS Ver.4.0 and HSPF Ver.12.0 (Bicknell *et al.*, 1985; 2001), which are conceptual-distributed hydrological behavior models provided free by U.S.EPA, were used to estimate river flow and sediment flux. Functions of the geographical pre-process, the hydrological database management and hydrological/hydraulic (one dimensional nonuniform flow) calculation scheme were packaged within the model. Also in the model, detached terrestrial sediment by rainfall and by gully erosion was transported to the river with surface runoff. Suspended and bed load with three assumed particle diameters (0.0025mm, 0.015mm and 1.0mm) in the river were calculated continuously. The modelling workflow, which is

shown in figure 5, were indicated by a simplified method using general geographic/ meteorological datasets and local observing datasets which may be enough for the regional scale prediction of hydrology and aquatic behaviour. The explanations of model calculations and its application scheme were detailed in the user's manual (Bicknell *et al.*, 2001) and references (Donigian, 1991).

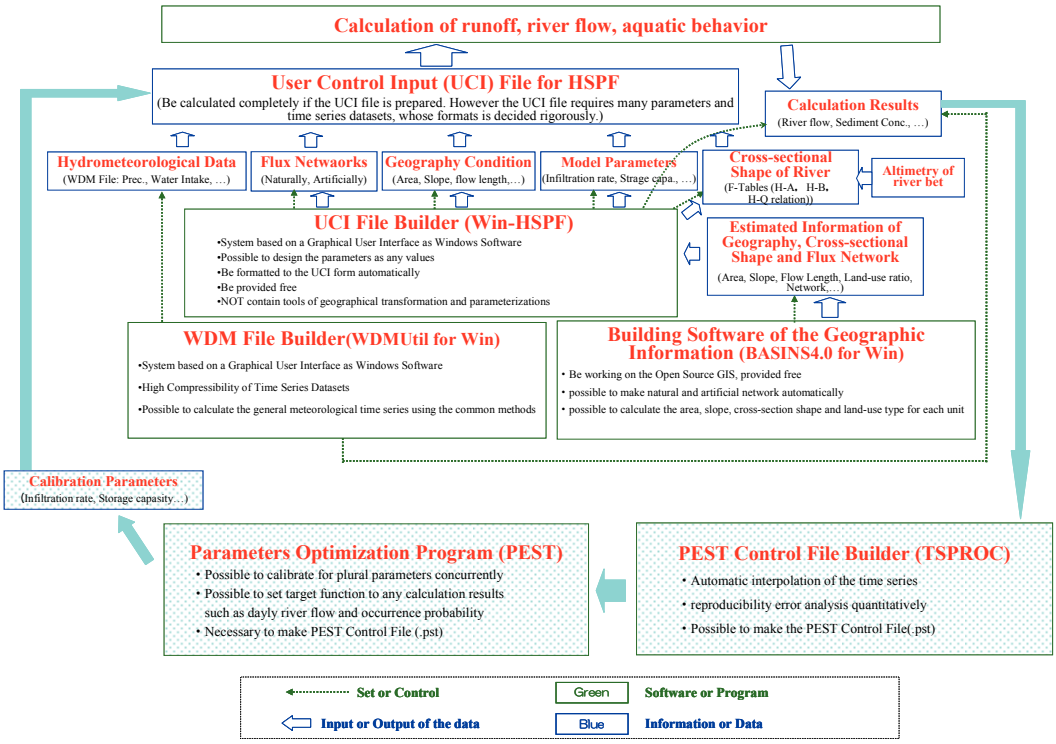

Figure 5: The modelling workflow indicated in simplified method using general geographic/meteorological datasets and local observing datasets.

As the first step, a natural flux network like a natural river with sub-basins separated with anastomosis points were automatically constructed using BASINS for the Yahagi River Basin. The watershed delineation tool, a BASINS extension, and the digital elevation model (Digital Map 50m, Geographical Survey Institute, Japan) were used to make river networks by setting to 20km^2 catchment area as upstream threshold. In the next step, automatic observing stations of water flow and water quality, water withdrawal points and consequent transportation of agricultural water, industrial water and drinking water, and dam/head works points accumulating runoff sediment were added as delineation points and artificial flux networks to natural flux network. Figure 6a shows sub-basins and flux networks on the landuse as a result of delineation. Moreover, each sub-basin was divided into six landuses (forest, paddy, farmland, city, barren and others; 1/10 Segmentalized Landuse, National Datasets of Japan) which were the minimum spatial unit used in runoff calculation. Figure 6b is a simplified conceptual diagram of delineated units for each sub-basins and its networks. As the results, the number of divided units became 344 for Pervious Land Segments (PLS, other than city), 74 for Impervious Land Segments (ILS, city) and 81 for Reach/Reservoirs (RCH, river).

As indicated by figure 5, geographical conditions such as area, slope, flow length and landuse property for each unit were calculated using BASINS and Win-HSPF. Additionally, hydrological parameters for each unit (landuse) were determined either by reference to empirically deduced values (U.S. EPA, 2000) or automatically calibrated using the method (PEST (Doherty, 2002) and TSPROC) mentioned figure 5. Parameter values used in this

research were listed in table 1.

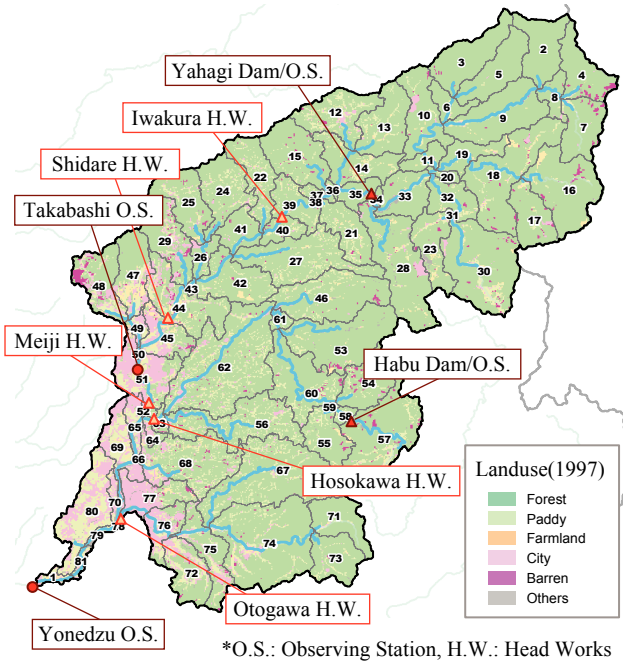

*O.S.: Observing Station, H.W.: Head Works

Figure 6a: Delineated sub-basins and flux networks in Yahagi River Basin.

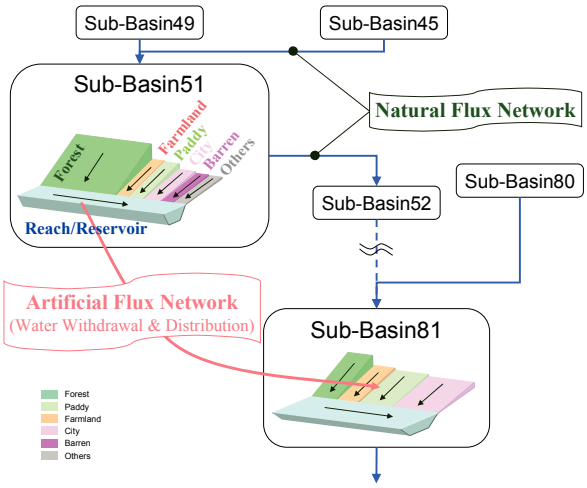

Figure 6b: Simplified conceptual diagram of delineated units for each sub-basins and its networks.

Table 1: HSPF modelling parameters used in this research

Group PWAT-PARM 1													
Name	CSNO	RTOP	UZFG	VCS	VUZ	VNN	VIFW	VIRC	VLE	IFFC	HHWT	IRRG	IFRD
All of the PLS	0	1	1	1	1	1	0	0	1	1	0	0	0

Name	Explanations	Unit	Land-use type without city and river				
			Forest	Paddy	Farmland	Barren	Othes
Group PWAT-PARM 2							
FOREST	Fraction forest cover	none	0.5	0.0	0.0	0.0	0.0
LZSN	Lower zone nominal soil moisture storage	mm	200.0	50.0	100.0	50.0	50.0
INFILT	Index to Infiltration Capacity	mm/h	5.0	1.0	3.0	3.0	3.0
LSUR	Length of overland flow	m	estimated value using BASINS, 60m-200m				
SLSUR	Slope of overland flow plane	–	estimated value using BASINS, 0.0001-0.4032				
KVARY	Variable groundwater recession	1/mm	0.0	0.0	0.0	0.0	0.0
AGWRC	Base groundwater recession	1/day	0.96	0.90	0.90	0.96	0.96
Group PWAT-PARM 3							
PETMAX	Temp below which ET is reduced	degC	4.44	4.44	4.44	4.44	4.44
PETMIN	Temp below which ET is set to zero	degC	1.67	1.67	1.67	1.67	1.67
INFEXP	Exponent in infiltration equation	–	2.0	2.0	2.0	2.0	2.0
INFILD	Ratio of max/mean infiltration capacities	–	2.0	2.0	2.0	2.0	2.0
DEEPFR	Fraction of GW inflow to deep recharge	–	0.0	0.0	0.0	0.0	0.0
BASETP	Fraction of remaining ET from baseflow	–	0.02	0.00	0.00	0.00	0.00
AGWETP	Fraction of remaining ET from active GW	–	0.0	0.0	0.0	0.0	0.0
Group PWAT-PARM 4							
CEPSC	Interception storage capacity	mm	3.8	2.5	2.5	0.0	0.0
UZSN	Upper zone nominal soil moisture storage	mm	5.0	2.0	2.0	1.0	1.0
NSUR	Manning' s n (roughness) for overland flow	complex	0.40	0.30	0.30	0.25	0.25
INTFW	Interflow inflow parameter	–	2.0	2.0	2.0	2.0	2.0
IRC	Interflow recession parameter	1/day	0.6	0.6	0.6	0.6	0.6
LZETP	Lower zone ET parameter	–	0.7	0.5	0.5	0.2	0.2

Group SED-PARM 1			
Name	CRV	VSIV	SDOP
All of the PLS	0	0	1

Name	Explanations	Unit	Land-use type without city and river				
			Forest	Paddy	Farmland	Barren	Othes
Group SED-PARM 2							
SMPF	Supporting management practice factor	none	1.0	1.0	1.0	1.0	1.0
KRER	Coefficient in the soil detachment equatio	complex	0.2	0.2	0.2	0.2	0.2
JRER	Exponent in the soil detachment equation	complex	2.0	2.0	2.0	2.0	2.0
AFFIX	Fraction of detached sediment storage decreases	/day	0.01	0.01	0.01	0.01	0.01
COVER	Fraction of shielded land surface from rainfall	none	0.5	0.5	0.5	0.0	0.0
NVSI	Rate of sediment entered to detached storage from atmosphere	kg/ha/day	0.001	0.001	0.001	0.001	0.001
Group SED-PARM 3							
KSER	Coefficient in the detached sediment washoff equation	complex	4.0	4.0	4.0	4.0	4.0
JSER	Exponent in the detached sediment washoff equation	complex	2.5	2.5	2.5	2.5	2.5
KGER	Coefficient in the matrix soil scour equatic	complex	4.0	4.0	4.0	4.0	4.0
JGER	Exponent in the matrix soil scour equation	complex	3.0	3.0	3.0	3.0	3.0

Group IWAT-PARM 1					
Name	CSNO	RTOP	VRS	VNN	RTLI
All of the ILS	0	0	0	0	0

Name	Explanations	Unit	Land-use type City
Group IWAT-PARM 2			
LSUR	Length of the assumed overland flow plane	m	100.0
SLSUR	Slope of the assumed overland flow plane	none	estimated value using BASINS, 0.0001-0.2633
NSUR	Manning's n for the overland flow plane	complex	0.05
RETSC	Retention storage capasity of the surface	mm	2.54
Group IWAT-PARM 3			
PETMAX	Temp below which ET is reduced	degree C	4.44
PETMIN	Temp below which ET is set to zero	degree C	1.67

Group SLD-PARM 1			
Name	VASD	VRSD	SDOP
All of the ILS	0	0	1

Name	Explanations	Unit	Land-use type City
Group SLD-PARM 2			
KEIM	Coefficient in the solids washoff equation	complex	1.0
JEIM	Exponent in the solids washoff equation	complex	1.8
ACCSDP	Rate of solids accumulation on the land surface	ton/ha/day	0.01
REMSDP	Fraction of removed solids from the storag	/day	0.01

Name	Explanations	Unit	Flow Network (River)
Group HYDR-PARM 2			
LEN	Length of the RCHRES (River)	km	estimated value using BASINS, 0.12-17.88
DELTH	Drop in water elevation from the upstream to the downstream	m	estimated value using BASINS, 0.1-370.9
STCOR	Correction to the RECHES depth to calculate stage	m	0.0
KS	Weighting factor for hydraulic routing	none	0.5
DB50	Median diameter of the bed sediment	mm	2.0, 10.0, 50.0 or 100.0 depend on the survey
Group SAND-PM			
D	Effective diameter of the transported sand particles	mm	1.0
W	Corresponding fall velocity in still water	mm/sec	150.0
RHO	Density of the sand particles	g/cm^3	2.65
KSAND	Coefficient in the sandload power function formula	complex	0.3
EXPSND	Exponent in the sandload power function formula	complex	4.0
Group SILT-CLAY-PM (silt)			
D	Effective diameter of the silt particles	mm	0.015
W	Corresponding fall velocity in still water	mm/sec	0.1
RHO	Density of the silt particles	g/cm^3	2.3
TAUCD	Critical bed shear stress for deposition	kg/m^2	0.01
TAUCS	Critical bed shear stress for scour	kg/m^2	1.0
M	Erodibility coefficient of the sediment	kg/m^2.hr	0.05
Group SILT-CLAY-PM (clay)			
D	Effective diameter of the clay particles	mm	0.0025
W	Corresponding fall velocity in still water	mm/sec	0.006
RHO	Density of the clay particles	g/cm^3	2.0
TAUCD	Critical bed shear stress for deposition	kg/m^2	0.01
TAUCS	Critical bed shear stress for scour	kg/m^2	1.0
M	Erodibility coefficient of the sediment	kg/m^2.hr	0.05

The relationship between water stage and flow quantity (*i.e.*, H-Q curve) based on the actual measurements was input as an F-Table for each river unit, which was divided by anastomosis point. Meteorological time series datasets including precipitation (hourly radar rainfall data, Japan Meteorological Agency (JMA)), air temperature, dew point temperature, wind speed and solar radiation (meteorological statistical information, JMA) were also input to the model, and an actual evapotranspiration time series from each land unit was evaluated from potential evapotranspiration using the HSPF. The time step/period of calculation was set to hourly in 2004, and estimation of river flow and sediment flux was targeted in this research.

3. Results and Discussions

Figure 7 shows the outflow time series of each runoff process (*i.e.*, surface runoff, intermediate runoff and base runoff) in the pervious land (alluvial fan) around the middle reaches from October 8th to 11th, 2004, when storm event occurred. Recognizable differences of outflow quantity depending on the runoff process in each landuse are indicated. While most water was surface runoff discharge in paddy field and city area, more than half of the total discharge was allocated to intermediate runoff in the forest. Therefore, the peak of outflow in paddy field and city area was two times higher than that in the forest. Annual outflow volume ratios of each runoff process are shown in figure 7. For the annual ratio of outflow, it was found that ratios of surface runoff and base runoff wildly differed in the landuse.

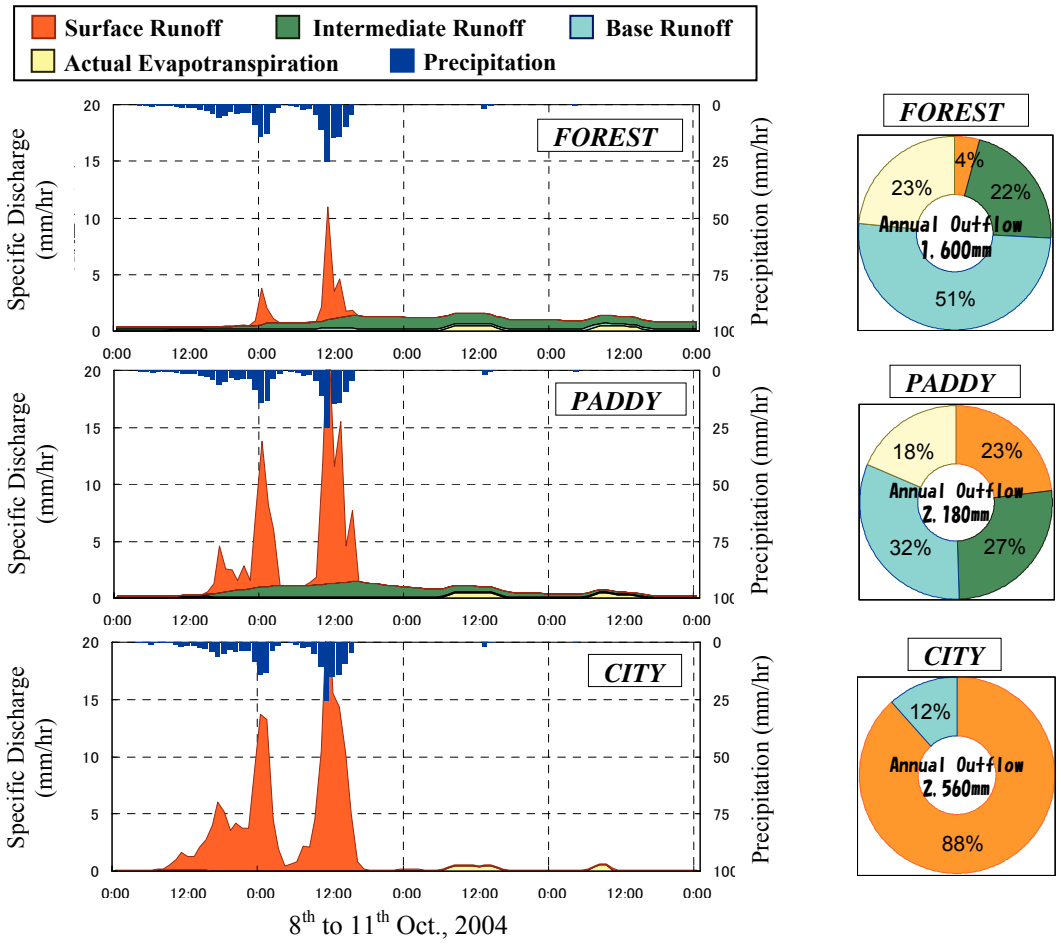

Figure 7: Outflow time series of each runoff process in the pervious land (alluvial fan) around the middle reaches in Yahagi Basin.

Relationships between calculated flow and observed flow in different river unit (*i.e.*, upstream and downstream) are illustrated in figure 8. Although comparatively high correlations (R^2>0.65) in every river unit are shown in the figure, a part of the flood flow in downstream is underestimated. Similar tendencies in various middle-down streams (Reach/Reservoirs) are also confirmed. These disagreements may be caused by the reproducibility error of surface runoff rate in areas other than forest.

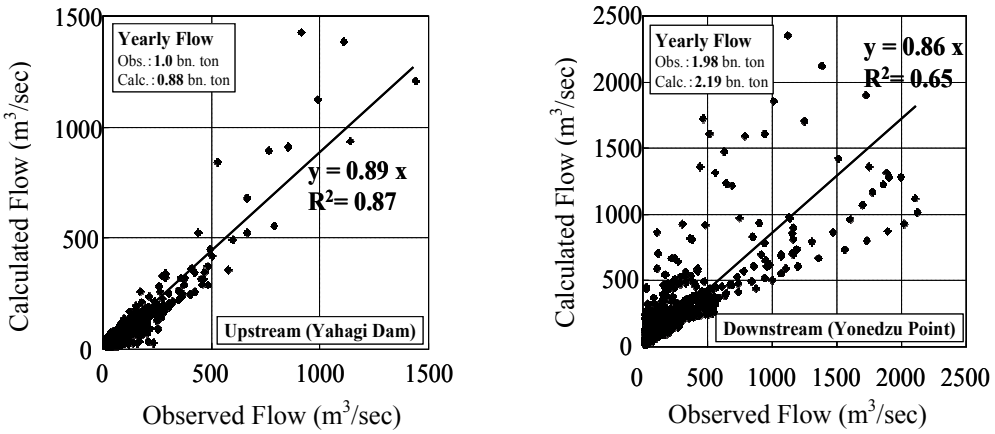

Figure 8: The relationships between calculated flow and observed flow.

At the same time, the relationship between sediment load and river flow (*i.e.*, L-Q curve) in the downstream (Yonedzu observing station) is shown in figure 9. Additional information, which was L-Q curve based on the automatic observation of turbidity and river flow in the same observing station (Kodama *et al.*, 2008), is also illustrated in the figure. Although calculated relations were identical with those of observation over a range of high sediment load (high river flow), calculated sediment load in normal flow conditions was overestimate because reproducibility of suspended load from river bed storage was inadequate. Therefore, the yearly sediment load (approx. 12 million tons) in downstream may be a relative overestimate. In future a study, it is aspired to estimate the ecosystem services based on the flux network analysis by improving some model settings.

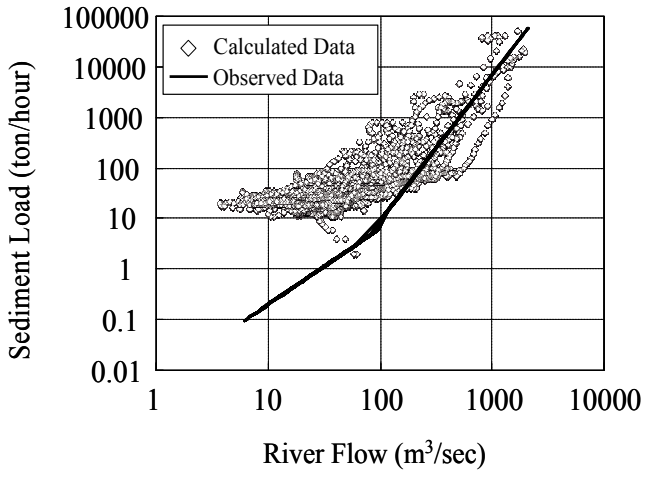

*Calculated sediment load express the value without sand particle component, since it was difficult to detect the large size particles as turbidity (NTU).

Figure 9: The relationship between sediment flux and river flow in the downstream (Yonedzu observing station).

4. Conclusions

Our goal was to use a semi-automated method (figure 5) of the watershed modelling to assess the river flow and the sediment load. It was possible to apply this method at various watershed locations, since the method does not require any cost or detailed input data or advanced techniques. In addition, results of an application to the Yahagi River Basin, outflow time series in the pervious land were calculated and recognizable differences depending on the runoff process were indicated. Although comparatively high correlations (R^2>0.65) between calculated flow and observed flow in every river segment were shown, a part of the flood flow in middle and down stream was underestimated. These disagreements may be caused by the reproducibility error of surface runoff rate in areas other than forest. Also, the calculated sediment load in normal flow conditions was overestimate because reproducibility of suspended load from river bed storage was inadequate, whereas calculated L-Q relations were identical with those of observation over a range of high sediment load (high river flow). In future a study, it is aspired to estimate the ecosystem services based on the flux network analysis by improving some model settings.

ACKNOWLEDGMENTS

The authors gratefully acknowledge the model and data purveyors, and financial support below. The hydrological dataset, observed flow time series in several river points, were provided by the Chubu Regional Bureau, Ministry of Land, Infrastructure and Transport, MLIT, Japan. Hydrological behavior models used in this research, the Hydrological Simulation Program FORTRAN (HSPF) and Better Assessment Science Integrating Point & Nonpoint Sources (BASINS), were developed and provided by the Environmental Protection Agency (EPA) and Stanford University, U.S.A. This research has been conducted as a part of the project entitled, “Research and Development in Assessment and Restoration for Eco-compatible Management of River Basin Complex around Ise Bay”, promoted by the Special Coordination Fund for Promoting Science and Technology for Sustainable National Land Management, MEXT, Japan.

REFERENCES

Aich Prefecture, Japan, http://www.pref.aichi.jp/0000008773.html in URL.

Agriculture, Forestry and Fisheries office of Nishimikawa region, Aich Pref. (2004), Annual report for water resource management in Yahagi river, *A Report of Aich Pref.*, 180p.

Bicknell, B. R., Donigian, Jr., A. S. and Barnwell, T. A. (1985), Modeling water quality and the effects of agricultural best management practices in the Iowa River Basin, *Water Sci. Technol.*, 17, pp.1141-1153.

Bicknell, B. R., Imhoff, J. C., Kittle, J. L., Jobes, T. H. and Donigian, A. S. (2001), Hydrological Simulation Program-Fortran user’s manual for version 12, AQUA RERRA Consultants and U.S. EPA, 845p.

Doherty, J. (2002), Manual of Model-Independent Parameter Estimation (PEST), *Watermark Numerical Computing*, 279p.

Donigian, A. S. (1991), Modeling of Nonpoint Source Water Quality in Urban and Non-urban Areas, *Rep. No. EPA/600/3-91/039*, AQUA RERRA Consultants and U.S. EPA, 94p.

Hanasaki, N., Kanae S. and Oki T. (2005), Global river discharge simulation taking into account irrigation water withdrawal, *Annual Journal of Hydraulic Engineering*, 49, pp.403-408. (In Japanese)

Kodama, M., Komatsu, Y., Okamoto, T., Kuroda, S., Arakawa, J. and Murakami, M. (2008), Effect of River Flow Regulation on Estuarine Environment, *Journal of Water and Waste Japan*, 50, pp.155-161. (In Japanese)

Nawarathna, B., Kazama S. and Sawamoto M. (2002), Evaluation of reservoir and irrigation effect on runoff simulations in the Mekong river basin, *Annual Journal of Hydraulic Engineering*, 46, pp.289-294.

Robert C., Ralph A., Rudolf G., Stephen F., Monica G., Bruce H., Karin L., Shahid N., Robert V. N., Jose P., Robert G. R., Paul S. and Marjan B. (1997), The value of the world's ecosystem services and natural capital, *Nature*, 387(15), pp.253-260.

Tebakari T., Yoshotani J. and Suvanpimol C. (2004), Effect of large scale dams on hydrological regime in the Chao Phraya river basin, Kingdom of Thailand, *Annual Journal of Hydraulic Engineering*, 48, pp.481-486. (In Japanese)

Toda, Y., Tsujimoto T., Ikeda T. and Tadakuma Y. (2006), Interaction between flow and growth of periphyton in sand river, *River Flow*, 2, pp.2073-2080.

Tsujimoto, T., Y. Toda, T. Tashiro, M. Obana, K. Sato and R. Tsubaki (2008), Study on strategic environmental assessment methodology for eco-compatible river basin management, *Advances in River Engineering*, 14, pp.367-372. (In Japanese)

Tsujimoto, T. *et al.* (2008), Research and Development in Assessment and Restoration for Eco-compatible Management of River Basin Complex around Ise Bay", *Research Report for the Special Coordination Fund for Promoting Science and Technology*, 135p. (In Japanese)

U.S. EPA (2000), Estimating Hydrology and Hydraulic Parameters for HSPF, BASINS Technical Note 6, *EPA-823-R00-012*, 32p.

Wongsa, A. and Shimizu Y. (2003), Modelling pre-channelization and their impact on flood and sediment yield in Ishikari river basin, *Annual Journal of Hydraulic Engineering*, 47, pp.223-228.

OB RIVER CHANNEL TRANSFORMATION DOWNSTREAM OF NOVOSIBIRSK HYDROPOWER PLANT (WEST SIBERIA, RUSSIA)

Konstantin Berkovich

Chief scientist, Scientific research laboratory for erosion and fluvial processes, Faculty of Geography, M.V.Lomonosov Moscow state university, Leninskiye gory, Moscow, 119991, Russia, e-mail: berkovitch@yandex.ru

ABSTRACT

Ob River channel transformation downstream of Novosibirsk hydropower plant is considered over a period of time as long as 40 years. The hydrological and hydraulic stream characteristics were revealed as well as riverbed and banks morphological and geological features. Process course is stated by water level changes. Rapid low-water level recession was found out over the first decade which became slower afterwards but did not stopped. That was unfavourable and even dangerous for municipal water supply facilities operation as well as for navigation and structures situated on the river banks. Continuing riverbed transformation is caused not only by bed degradation that is typical downstream of large dams but else by underwater alluvium mining.

Keywords: tail water section of waterworks facilities, riverbed processes

1. INTRODUCTION

One of dramatic problem of large waterworks facilities operation is continued through decades water level recession. It causes often the conflict situation in river utilization downstream of large dams. Water level lowering makes difficult water supply points operation, results in depth reduce and navigation trouble, river banks and structures on them destruction, floodplain aridization. As happens the prognosis does not prove to be correct. It requires serious riverbed processes monitoring and complex approach to practical tasks solution though individual for specific rivers.

Novosibirsk Hydropower Plant was put into operation in 1961. The dam as tall as 18 m made the reservoir with the volume by normal pool level 8.8 km^3. Useful reservoir volume is 4.4 km^3. Waterworks facility is counted on average annual discharge as large as 1660 m^3/s to be released.

Ob River bed transformation turned out to be unfavorable for numerous structures: wharfages, water supply, navigation, as early as in early 1970-s, in less than 10 years after dam was constructed. Due to intense unforeseen by project water level lowering, water supply facilities operation was complicated. To clear up the causes of this effect the riverbed transformation complex research was fulfilled in 1976-1978 (Berkovich, Vexler et al., 1981). At the time, water level fall prognosis was elaborated up to 2000 considering either mining stoppage or continuation. But despite some taken measures, level fall continued to drop. Level recession turned to be more than forecasted one what resulted in new complication in water supply operation at the beginning of XXI century. The cause of convergence forecasted and observed riverbed state downstream of large dams is very often inadequate taking into account some natural riverbed features and human induced disturbances.

Riverbed transformation downstream of large dam evolves under the influence of two groups of factors: common for most part of dams and local that are typical for individual river reach. The first include run-off regulation provided by project as well as sediment storage into reservoir and daily water discharge fluctuation resulting from power plant operation. The local factors are riverbed geological structure and its change along the river, bed sediment composition as well as man-made riverbed disturbance fallen at the same time that dam operation.

N.I. Makkaveev (1957) pointed out how important is to take into account geological riverbed structure analyzing channel transformation downstream of large dams. Human impact strengthening in 1970-1980-s in many cases resulted in inadequacy of forecasts which had been elaborated while dams have been projecting. Ob riverbed underwent severe changes within few decades after Novosibirsk dam was constructed. Dam adjacent portion of river lies within the precincts of the one of largest Siberia's cities. It is overburden with different structures: water supply facilities, wharfs, bridges, underwater pipe crossings, river engineering structures. Therefore riverbed subsequent evolution evaluation is of great practical importance.

2. RIVERBED TRANSFORMATION FACTORS

2.1. Hydrological Characteristics

To assess the changes in hydrological characteristics the data of two main gauges were used: Dam gauge (0 km) and Novosibirsk gauge (20 km from the dam), as well as Dubrovino gauge situated in 110 km from the dam. Due to little useful volume, Novosibirsk reservoir fulfils rather modest seasonal run-off regulation. Regulation coefficient represented as reservoir useful volume to flood volume (19.2 km^3) ratio is just 0.14. Nevertheless flood run-off decreased to 20-25%, whereas winter run-off increased to 10-12%. So run-off regulation resulted in spring-summer flood peak reduction. Mean flood discharge over the dam operation time is 3900 m^3/s, maximum one 9600 m^3/s. The tendency toward flood reduction is observed: within last 20 years maximum discharge has not exceeded 5600 m^3/s, whereas natural one exceeded 12000 m^3/s. Run-off distribution change can be observed as far from the dam as 300 km.

Sediment load changed much more significant. Suspended sediment load at Novosibirsk gauge decreased from 14 mln to 4 mln tons per year, mean annual turbidity - 3.5-fold – from 247 to 71 g/m^3. The major part of suspended sediment runs in Spring (80%). Bed sediment load stops in reservoir entirely. It is fixed that before dam was constructed, 4.5 mln tons of suspended sediment were deposited annually within 180-km-long river section submerged at present by reservoir. At the same time, suspended sediment load increased downstream of Novosibirsk in a section as long as 450 km only on the account for large tributaries flowing into. Without taking into consideration sediment contribution from tributaries it is clear that Ob River itself lost in this section as much of suspended sediment as nearly 3 mln tons a year. Thus the natural tendency of Ob River longitudinal profile evolution was aggradation (Makkaveev, Chalov, 1963) It is confirmed by minimum water level rise before dam was constructed which amounted 25 cm in first half of XX century. Calculated bed sediment load was about 1.4 mln tons a year or 10% of entire sediment load at a time (Chalov et al, 1999).

Bed sediment load changed after reservoir formation. According to the most recent sand waves movement measurement (in 2000-s) in the distance 12-30 km from the dam, bed sediment load is at average 550 thousand tons per year. Near the dam, almost all bed sediment load results at present from bank failure because incision practically stopped. Alluvial layer

was washed out for the most part and flow contacts directly with rock bed. There are some local base levels (Rock cape). Suspended sediment deficiency is observed as far as few hundred kilometers downstream.

Daily release waves movement can be noted in a section as long as 100 km downstream of dam. The waves are most distinct in dam-adjacent section as long as 30-40 km. Maximum wave amplitude over open channel period is 70 cm, their movement velocity 12 km/h. The more wave amplitude the more quickly it spreads flat. The wave 70 cm high is reduced up to 10 cm within 40-km-long section of river. Wave movement is related to flow velocity increase. Wave as high as 70 cm results in 25-40% maximum velocity increase. Bottom velocity change amplitude when wave goes through is 0.53 m/s in 6 km and 0.35 m/s in 14.5 km from the dam.

2.1 Geological Condition and Channel Morphology

Main natural factor determinative local riverbed transformation specific character is complex valley, channel, banks geological structure (fig. 1). River crosses few granite massifs in a section as long as 100 km. High position of Paleozoic rock presented by sandstone and slates connects with granite outcrops. They form river terraces base and come to light in riverbed as the granite do. Rocks lie directly under bottom and floodplain as on the right as left banks in dam-adjacent section which coincides with city borders. Rock roof is uneven: there are projections and depressions as deep as 8-10 m and more. Alluvium layer thickness covering rocks is at average 0.5-3.5 m. Outside 30-km-long dam-adjacent section, rocks appear in the base of the right bank, form stony caps. Rocks prevent from bed erosion in dam-adjacent section whereas outside of it they only tell on some features of horizontal deformation and don't limit vertical one.

2.2 Anthropogenic Factors

Human induced riverbed disturbances have played significant role in Ob riverbed recent evolution. Main disturbances are sand and gravel underwater mines and river engineering works (dredging etc). Besides the bridges, dikes, embankments and other structures are widespread. This factors come often on foreground and shade the natural factors activity.

Extensive works aimed navigation improvement had been fulfilled in 1960-1980-s. Dredging workload equaled 20-50 thousand m^3 from 1 river kilometer. The guaranteed depth was risen from 1.7 m in 1966 to 2.5 m in 1991. Dredging volume reduced somewhat after 1992-1993 as a result of economical crisis. Over recent 12 years, dredging volume amounts just about 4 thousand m^3/year from 1 km. However much reduced dredging is now the main measure to maintain navigation depth 2.3 m.

The most strong anthropogenic factor determining riverbed transformation is underwater sand and gravel mining. Sand and gravel had mined directly within city borders in 1960-1982. Altogether more than 25 mln m^3 of alluvium had been moved off in 40-km-long river section downstream of dam up to 1982. In 1980-1990-s underwater mines elaborated in 65-85 km from the dam where more than 30 mln m^3 had been moved off. Despite prohibition some mines have been elaborated in 2000-s in 20-25 km from the dam where 4-5 mln m^3 was moved away. The consequences of intense mechanical change of riverbed tell on up to now.

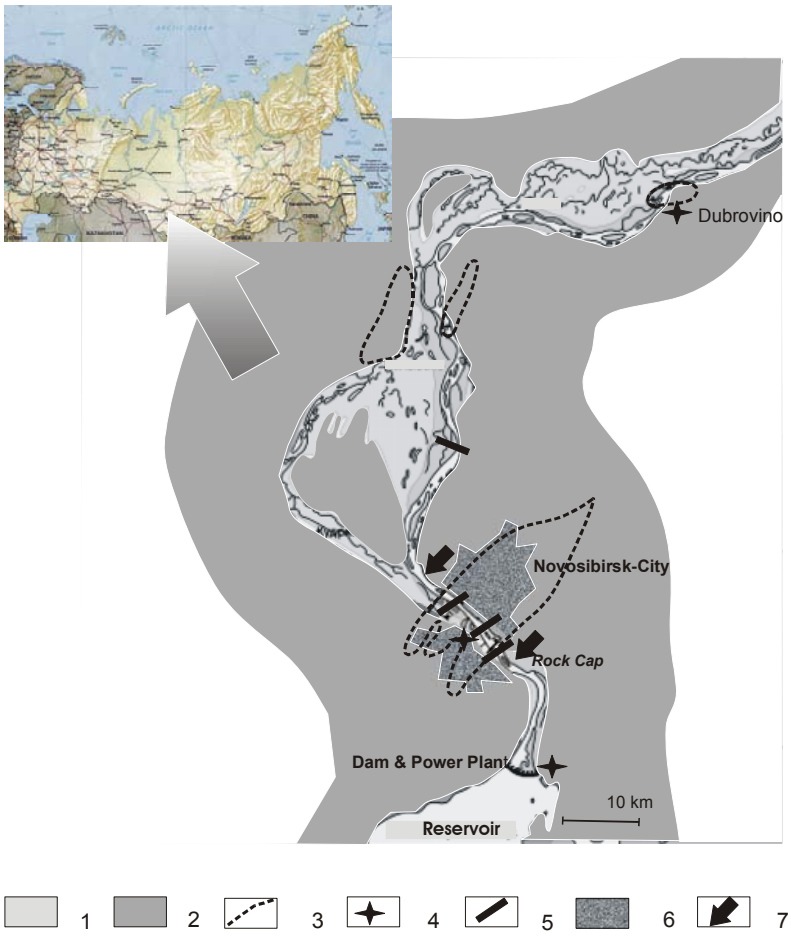

Fig. 1 Scheme of Ob riverbed section downstream of Novosibirsk dam (map of Russia from the site: www.itlibitum.com)
1 – floodplain; 2 – terraces, Plateau and uplands slopes; 3 – granite massifs; 4 – hydrological gauges; 5 – bridges; 6 – city and settlements; 7 – main water supply facilities.

3 OB RIVER CHANNEL TRANSFORMATION

3.1. Channel Characteristics

In spite of the complex geological structure bed sediment size was relatively small under natural conditions. Mean particle size equaled 0.2-0.3 mm increasing up to 0.5 mm near rock outcrops. Correlation of gradient and bed sediment size shows that Ob riverbed was low stable and notable for high intensity of local periodical deformations.

Natural riverbed pattern was mainly braiding what was related to low bed stability, easy river banks erosion, run-off irregularity, relatively large sediment load with the tendency to its deposition. Riverbed pattern was unequal along the river. In the dam-adjacent section, channel was relatively narrow, straight with some riverside branches, prevalent part of the flow concentrated in one main branch. There were many shoals, rock outcrops, narrow floodplain. Further downstream channel is divided mostly to two main branches by central island. Water discharge and sediment load in them periodically altered but main branch always took no more than 40-50% of general discharge. Also there were some low-water riverside branches. Owing to low bed stability central and alternative bars were the prevalent bed forms under natural conditions. The alternative bars often seized from the banks as they moved.

3.2 **Water Level Recession**

The most evident attribute of riverbed transformation downstream of large dam is water level recession (fig. 2). It is one of the heaviest consequence of reservoir influence by the intense hydroeconomic and transport use of the river as it influences water supply facility operation, bridges, embankments and dam itself firmness, waterway condition. Rapid low-water level recession is characteristic downstream of Novosibirsk dam. Initially it was strikingly revealed near the dam – in tail-water zone. Compared to natural state low-water level recession equaled 1.5 m by 1975 by water discharge less than 2000 m^3/s and 1.2 m by discharge 2000-6000 m^3/s. Mean level recession rate amounted about 7 cm/year over the period 1959-1975. Later level recession became slower: in 1976-1986 it amounted 28 cm or 3 cm/year by low-water discharge 1300 m^3/s. Still slower was level recession in 1987-1998 when its rate reduced to 1 cm a year. By 2005 total level recession by discharge 1300 m^3/s run up to 1.86 m.

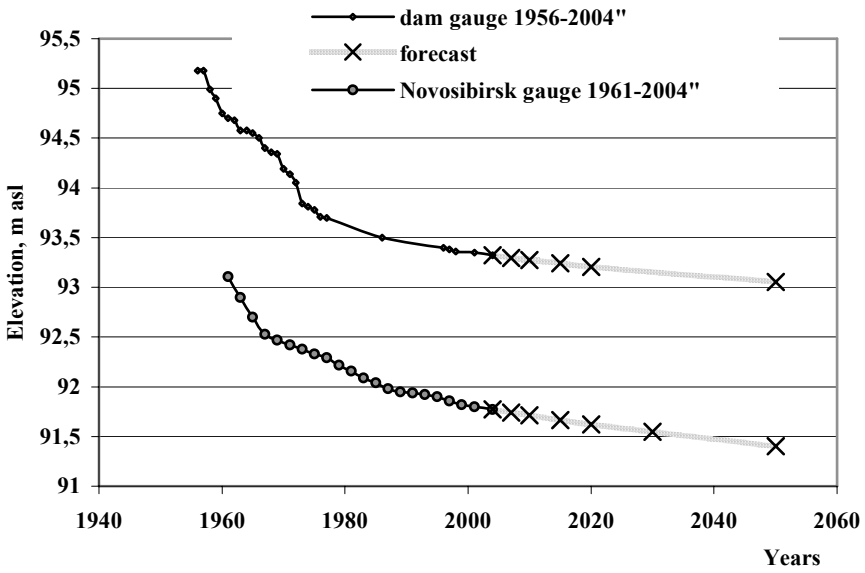

Fig. 2 Level recession and its prognosis at Dam and Novosibirsk gauges for discharge 1300 m^3/s

Though lesser in magnitude level recession was observed at Novosibirsk gauge situated in 20 km downstream of the dam. Level recession by discharge 1300 m^3/s amounted 0.5-0.6 m by 1975 and 1.32 m by 2005. Recession rate reduced here as well: in 1961-1967 recession rate was as high as near 10 cm/year, in 1968-1987 – 4,5, later – 2 cm/year.

It is characteristic that riverbed degradation due to hydrological regime alteration changes over time according to the relationship (Simon, 1995):

$$z = z_0(t)^m \qquad (1)$$

where z – bed or water surface elevation over period of time t (years) after disturbance, z_0 – initial elevation, b, m, k – empirical coefficients. This and similar relationships can serve to forecast subsequent riverbed changes on the assumption of empirical coefficients correct definition on the base of field observation.

Ob River level recession at Dam gauge by discharge 1300 m^3/s over the period 1956-2005 describes with relationship:

$$H = 95{,}66t^{-0{,}0061} \quad (2)$$

in 20 km downstream (Novosibirsk gauge):

$$H = 93{,}42t^{-0{,}0042} \quad (3)$$

where H – level elevation, t – time (since 1956); correlation coefficient is 0,955. It is clear that though level recession develops quite regular it goes out very slowly.

3.3 **Riverbed Degradation and Channel Forms Change**

The cause of water level recession is bed degradation, its expansion downstream as well as channel's morphology and geometry influenced run-off regulation. Bed degradation established on the base of river maps analysis advanced strongly: within first years (1957-1960) degradation volume amounted in dam-adjacent section near 10 mln m^3. It corresponded to mean bed elevation lowering 10-12 cm/year. Channel capacity increased by 22 mln m^3 in 1973, 10 mln m^3 in 1985 and 8.2 mln m^3 in 2004 (fig. 3). In sum volume of material washed away came to 50 mln. m^3, or at average near 1 mln m^3 per year. Almost a half of this amount falls on material moved off out of underwater mines.

Degradation advanced nonuniform along dam-adjacent section of the river what is stated by mean depth changes in individual fixed cross sections (tab. 1).

Table 1 Mean Ob River depth change downstream of dam

Distance from the dam, km	Mean reduced depth (m) in years				
	1961	1967	1975	1987	2004
0-10	1,67		2,99		3,21
10-30		2,42	3,35	3,7	3,71

In 1959-1975, mean depth reduced to the same level increased more rapidly near the dam; later it increased slightly. The most depth increase in the section 10-30 km from the dam was noticed in 1967-1987, whereas later the depth did not increase there. Mean depth increase was accompanied by cross section shape change. The mean to maximum depth ratio increased at average from 0.4-0.5 in 1967 to 0.65-0.7 in 1985.

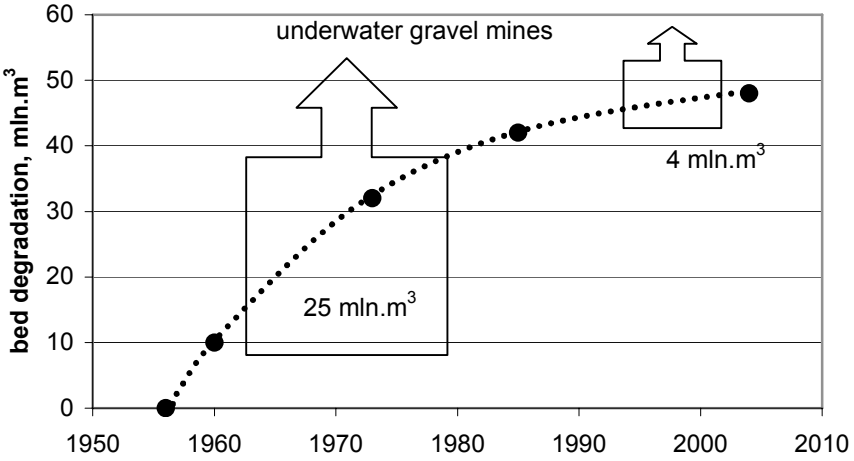

Fig. 3 Riverbed degradation and underwater mines volume in the section 0-30 km from the dam

Though underwater mining was stopped in early 1980-s, riverbed degradation went on. It stopped only locally in some spots where flow reached rock bed. Degradation volume near the dam (0-10 km) amounted in 1985-2004 as much as 2.8 mln m^3, what corresponds to the mean eroded layer 0.45 m. Further downstream (10-30 m) mean eroded layer exceeded 0.6 m. As a result, bed sediment size increased very much: it amounted in dam-adjacent section 1.4-6.6 mm.

One-directional riverbed deformation are noted far beyond the bounds of dam-adjacent section. Detailed river maps (1985 and 2004) comparison made clear that erosion prevailed in the section as long as 100 km and its rate amounted near 5 thousand m^3 per year from 1 river kilometer. At that two sections are notable for erosion predominance and one for deposition one. First erosion section extends 60 km from the dam and has mean erosion rate 7 thousand m^3 per year; the second one is remote by 80-100 km from the dam with mean erosion rate 12 thousand m^3 per year from 1 river kilometer. In between the section as long as 20 km lies where deposition prevails amounting 9 thousand m^3 per year from 1 river kilometer (fig. 4). Sediment size here is noticeable less amounting to 0.8-1.2 mm. The second erosion section origin and its large deformation rate is related to the fact that deformation here does not constrain by rock outcrops in riverbed.

Few distinctive features of one-directional deformation revealed within all 100 kilometer-long section downstream of the dam: 1) disappearing of some riverside low-water branches and main stream concentrating in remained ones, bifurcation system rebuilding; 2) rapid new floodplain forming by the armlets bifurcation and junction points as well as in secondary branches; 3) meandering development in main branches.

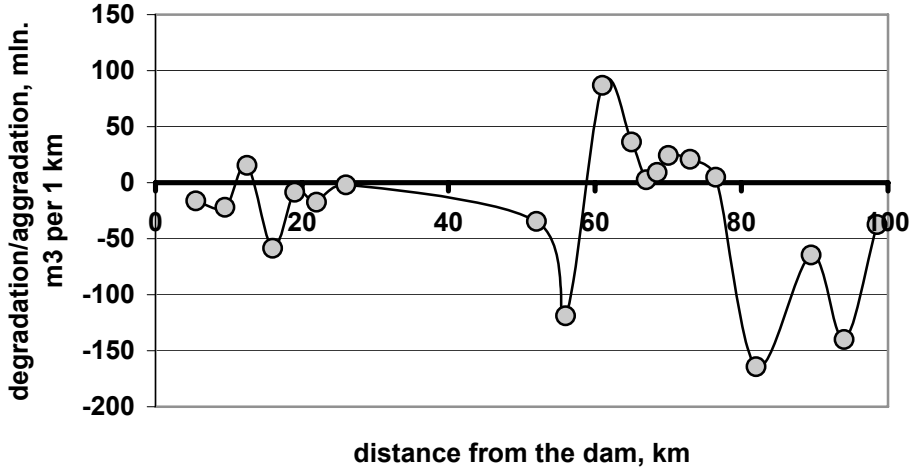

Fig. 4 One-directional Ob riverbed deformation within 100-kilometer-long section downstream of the dam over the period 1985-2004.

Some secondary arms dying out began as early as in 1960-1970-s. Numerous large islands united with floodplain. At that the largest and fullest branches developed concentrating predominant portion of discharge. Main (navigable) river branches' relative water capacity equals at a present 60-80% during flood and up to 90% over low-water period whereas in 1970-s it did not exceed 40%. Discharge redistribution to navigable branches was stimulated by sand bar mobility decrease and their strengthening with vegetation as well as river engineering and dredging course through few decades.

River geometry changed significantly through last 30 years. Open low-water channel width reduced from 1140 m in 1976 to 850 m in 2004, islands area increased.

It is typical for Ob riverbed forms: low surface elevation and little seasonal changes; vegetation overgrowing on their elevated parts; flatness of their longitudinal profile. Elevated 1-2 m below low-water level, majority of alternative and central bars became underwater. It is related to the sediment load decrease as well as to flood level reduction. High elevated bed forms overgrow with shrubs and grass and became new floodplain. Bed form size increased as compared to natural conditions, what is corresponding with channel stability increase and its morphology change.

The prognosis of riverbed subsequent changes is of great significance for all water-users of Novosibirsk-city and first of all for water supply system, uninterrupted operation of which depends on water level and the latter – on riverbed transformation direction and rate. To elaborate the prognosis of water level recession the relationships (2, 3) were used. Exponent *m* changes over time were taken into account.

The calculation makes clear that level recession near the dam will amount by 2020 further 15 cm (by discharge 1300 m^3/s), and 30 cm by 2050 as compared to present value (fig. 2). Level recession in Novosibirsk will equal 18 cm by 2020 and 40 cm by 2050. It is remarkable that since 2010 water level according to mentioned discharge will not satisfy regular municipal water supply facilities operation and their radical reconstruction requires.

3. CONCLUSIONS

Novosibirsk waterworks facility have caused seasonal run-off irregularity decrease, sediment load reduction and unsteady flow movement rise downstream of the Power Plant. In turn, underwater sand and gravel mining caused riverbed transformation acceleration. Riverbed degradation and man induced disturbance resulted in water level recession which

has lasted few decades. Though slowing down it does not cease even when river bottom becomes firm against washing out. It should be taken into consideration when water supply facilities, bridges, underwater pipe crossing, embankment and other structures projecting and reconstructing.

ACKNOWLEDGMENTS

Accomplished at financial support of Russian Foundation for Basic Research, Grant No 07-05-00421, Ob River basin state authority of waterways and navigation as well as Upper Ob river basin water resources authority.

REFERENCES

Berkovich, K.M., Vexler A.B. et al. (1981) Ob River channel forming downstream of Novosibirsk hydropower plant, in *Proceeding of West Siberian Hydrometeorological scientific Institute*, 52, pp. 3-20 (in Russian).

Makkaveev, N.I. (1957) Riverbed processes and waterway works downstream of dams, in *Transactions of Central Institute of Water Transport*, XII, pp. 5-86 (in Russian).

Makkaveev, N.I., Chalov, R.S. (1963) On morphological indication of contemporary aggradation in river valleys, in *Proceedings of the Academy of Sciences, geography series*, 3, pp. 25-35 (in Russian).

Chalov, R.S., Lu, Shuguang, Alexeevskiy, N.I. (1999) Sediment transport and channel processes in large rivers of Russia and China, 212 p, Moscow State University, Moscow (in Russian).

Simon, A. (1995), Energy, time, and channel evolution in catastrophically disturbed fluvial system, *Geomorphology*, 12, pp. 215-232.

SPATIAL DISTRIBUTION OF RUNOFF DISCHARGES CONSIDERING WADI CHANNEL FLOW WITH UPSCALING TECHNIQUE BASED ON HOMOGENIZATION THEORY

Mohamed Saber[1], Toshio Hamaguchi[2] and Toshiharu Kojiri[3]

[1]PHD Student, Department of Urban Management, Kyoto University, e-mail: saber@wrcs.dpri.kyoto-u.ac.jp
[2] Assistant Professor, DPRI, Kyoto University, e-mail:Hamaguch@wrcs.dpri.kyoto-u.ac.jp
[3]Professor, Disaster Prevention Research Institute, Kyoto University, e-mail: tkojiri@wrcs.dpri.kyoto-u.ac.jp
Disaster Prevention Research Institute, Gokasho, Uji, Kyoto, Japan, 611-0011

ABSTRACT

It has been stated that the limitation of the development of arid zone hydrology is the lack of high quality observations. This paper introduces a distributed hydrological model of the Wadi system for flood control and water resources management considering the discontinuous occurrence of flow in both space and time. We provide a homogenization method of upscaling hydrologic parameters related to a distributed runoff model from macroscopic aspects up to megascopic ones. Discharge distribution of the Wadi system can be simulated. Transmission losses and their effects on surface and subsurface flow are evaluated. The conjunctive use of surface and subsurface water is recommended. It is concluded that this model is an applicable methodology for distributed discharge in the arid regions.

***Keywords*:** Homogenization theory, transmission losses, Wadi system and Kinematic wave model

1. INTRODUCTION

Understanding of hydrological processes of Wadi system in the arid regions is so needed due to the importance of the water resources. In the arid regions, there are many problems; the shortage of water resources and increasing the losses. Despite the critical importance of water in arid areas, hydrological data have historically been severely limited. Moreover, those countries of the arid areas are facing the problem of overpopulation, and consequently the demand of water resources for the agricultural and domestic use.

This study proposes a homogenization method of upscaling hydrological parameters related to a distributed runoff model from microscopic aspects up to macroscopic ones. Homogenization is a mathematical method that allow us to upscale differential Equations. The essential idea of homogenization is to average inhomogeneous media in some way in order to capture global properties of the medium.

Wheater et al. (1997) and Telvari et al. (1998) stated that surface water and groundwater interactions depend strongly on the local characteristics of the underlying alluvium and the extent of their connection to, or isolation from, other aquifer systems. Transmission losses in semiarid watersheds raise important distinctions about the spatial and temporal nature of surface water–groundwater interactions compared to humid basins. Ephemeral streams are characterized by much higher flow variability, extended periods of zero surface flow and the general absence of low flows except during the recession periods immediately after moderate to large high flow events (Knighton and Nanson, 1997).

Our main purpose is developing distributed hydrological model to overcome the prescribed struggles for water resources management and flood control in Wadi system due to the deficiency of the water resources and the dangerous of the flood threat. In addition to,

studying the interaction between surface and subsurface water.

2. THE TARGET WATERSHED

We aim to study Wadi Assiut watershed (Figure 1) which is located in the Eastern Desert of Egypt. It is located between Long: 32°30′ E & 31°12 W ′ and Lat: 27°48′ N & 27°00 S ′. The total area of Wadi Assiut Catchment is 7293 km2.

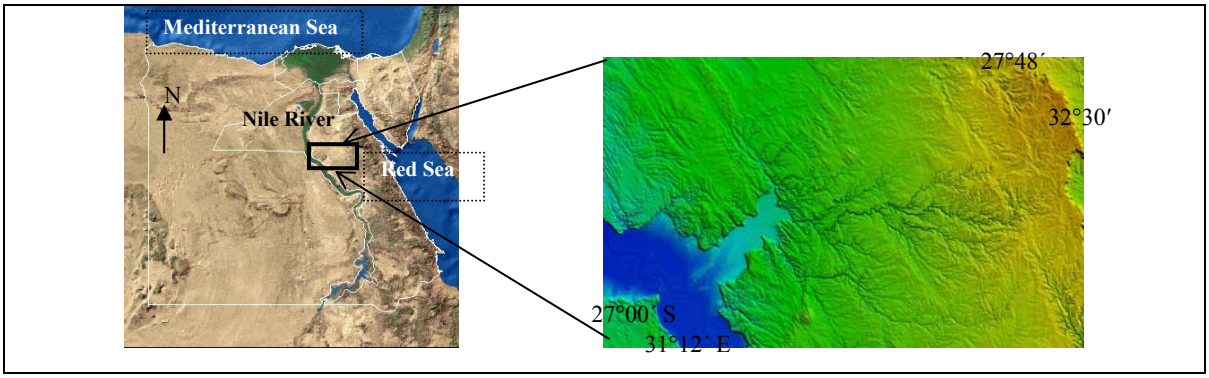

Figure 1 Location map of Wadi Assiut Watershed, Egypt

It is characterized by the features of Wadi System. The establishment of new town there which will be in the near future crowded by populations, thus the hydrological modeling for water resources management and flood threat control is urgently needed and crucial.

3. CHARACTERISTICS OF WADI SYSTEM

The arid regions are characterized by the expanding populations, increasing per capita water use, and limited water resources and so on. Rainfall is characterized by extremely high spatiotemporal variability. The most obvious characteristics in the ephemeral streams are the initial, transmission losses and the discontinuous occurrence of flow in both space and time.

3.1 Initial and Transmission Losses

Initial losses occur in the sub-basins before runoff reaches the stream networks, whereas transmission losses occur as water is channeled through the valley network. Initial losses are related largely to infiltration, surface soil type, land use activities, evapotranspiration, interception, and surface depression storage. Transmission losses are important not only with respect to their effect on stage flow reduction, but also to their effect as recharge to groundwater of underground alluvial aquifers. It was suggested that two sources of transmission loss could be occurring, direct losses to the bed, limited by available storage, and losses through the banks during flood events as shown in Figure 2A.

3.2 Surface and Subsurface Water Interactions

Surface water–groundwater interactions in semiarid drainages are controlled by transmission losses. In contrast to humid basins, the coupling between stream channels and underlying aquifers in semiarid regions often promotes infiltration of water through the

channel bed, i.e. channel transmission losses (Stephens, 1996; Goodrich et al., 1997). The balance between distributed infiltration from rainfall and Wadi bed infiltration is obviously dependant on local conditions, but soil moisture observations from S.W. Saudi Arabia imply that, at least for frequent events, distributed infiltration of catchment soils is limited, and that increased near surface soil moisture levels are subsequently depleted by evaporation.

4. METHODOLOGY AND MODEL COMPONENTS

Due to the severe problems of Wadi system in the arid areas, it is recommended to develop the distributed hydrological models, including surface water/groundwater interactions in the active Wadi channel, sediment transport and evaporation processes. These are challenging studies, with particularly challenging logistical problems, and require the full range of advanced hydrological experimental methods and approaches to be applied.

A distributed hydrological model in the Wadi system is proposed. This model is based on the modification of Hydro-BEAM (Hydrological Basin Environmental Assessment Model), it was first developed by Kojiri et al. (1998). which has been chosen for simulation the surface runoff model and estimation of the transmission losses.

Thus, our approach is an integrated numerical model (Figure 2B) based on sporadic precipitation and under conditions of data deficiency where we developed the watershed modeling by using GIS tool, surface runoff and stream routing modeling based on using the Kinematic wave approximation, the initial and transmission losses modeling were estimated with applying SCS method (1985) (an empirical model for rainfall abstractions suggested by the U.S Soil conservation Service) and Walter's Eq. (1990) respectively, and groundwater modeling based on the linear storage model.

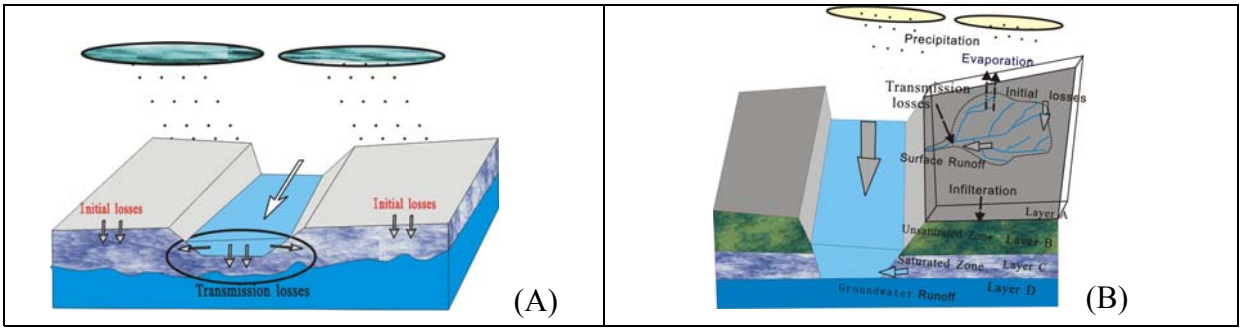

Figure 2 (A) Conceptual model showing transmission and initial losses in the Wadi System, (B) Schematic conceptual model of Wadi system

We provide a homogenization method of upscaling hydrologic parameters related to a distributed runoff model from macroscopic aspects up to megascopic ones. A surface flow direction prescribed through a flow routing map is significant to replace the discontinuous flow in the lumped model cell to the homogenized equivalent flow for the simplicity of calculations in the complicated Wadi system based on the conservation of water balance. Where the homogenized parameters (equivalent roughness coefficient n^* and equivalent hydraulic conductivity k^*) are equivalently derived from the mathematically formulated descriptions based on the conservation of surface and subsurface water quantities (Hamaguchi et. al., 2007).

The original Hydro-BEAM model that uses for the humid conditions can be adopted for simulation of Wadi system in the arid area as described in the following sections. Initial

and transmission losses are evaluated. The watershed to be investigated is divided into an array of unit mesh cells. A mesh cell can be arranged as a combination of a surface layer and several subsurface layers. The following description considers Hydro-BEAM calibrated with four subsurface layers, labeled A, B, C and D. A-Layer is calibrated using Kinematic wave model for the overland flow evaluation and the other C-D layers (subsurface layers) are calculated by the linear storage model.

4.1 Watershed Modeling

The watershed basin delineation and stream network determination are achieved using the digital elevation map (DEM) as input to Arcview GIS (Figure 3A), in addition to geomorphologic features can be calculated. We considered some points in the watershed modeling: i) Determination of the watershed boundary location, ii) Division of the watershed into a regular grid of mesh cells (2 km), iii) Determination of a flow routing network based on mesh cell elevation as given by a DEM.

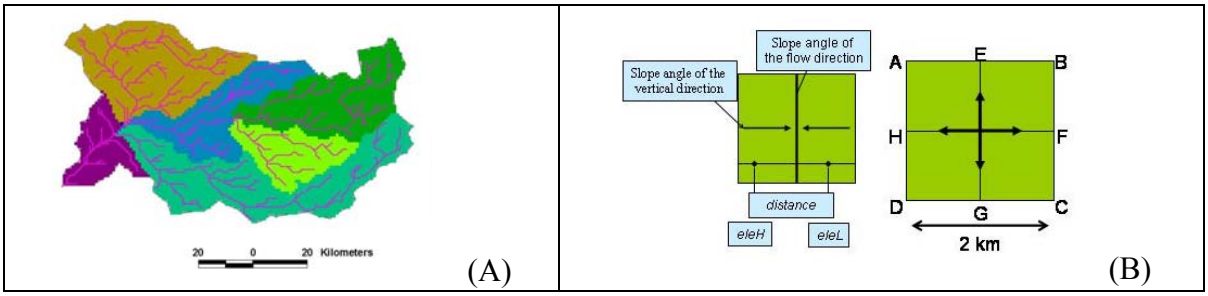

Figure 3 (A) Watershed delineation and stream network determination of Wadi Assiut, (B) Schematic diagram of the flow direction determination

There are two types of ***flow routing system***; 4 directions and 8 directions to determine drainage of flow water direction. Hydro-BEAM was originally developed to use a 4-direction flow routing map. Flow direction from any given mesh cell can be estimated using the DEM elevations of the corners of each mesh cell as declared in Figure 3B. Hydro-BEAM is set to use *five categories of land use types*. The land use distribution data (GLCC; Global Land Cover Characterization) are reclassified into 5 types.The five categories of land use types are; *mountains and forests, paddy field (rice field), desert, urban and water*.

4.2 Climatic Model

By using the metrological data of NCDC (National Climatic Data Center) , Global Hourly and Monthly data, ***Thornthwaite method*** can be adopted to calculate daily mean potential evapotranspiration as given in equations 1, 2, 3, and 4. The mean air temperature and duration of possible sunshine of each mesh are needed as meteorological data for our model.

$$E_p = 0.553 D_0 \left(\frac{10 T_i}{J} \right)^a \tag{1}$$

$$a = 0.000000675 J^3 - 0.0000771 J^2 + 0.01792 J + 0.049293 \tag{2}$$

$$J = \sum_{i=1}^{12} \left(\frac{T_i}{5} \right)^{1.514} \tag{3}$$

$$E_a = M \times E_p \tag{4}$$

Where, E_a *and* E_p *(mm/d)* are the actual and the potential evapotranspiration; *Ti* (^0C) is the monthly average temperature, *J*: Heat index, D_0 *(h/12h)* is the potential day length and *M* is the reduction coefficient, vapor effective parameter.

4.3 Kinematic Wave Model

The kinematic wave equations as given in eq. 5 are derived from the St. Venant equations by preserving conservation of mass and approximately satisfying conservation of momentum. The momentum of the flow can be approximated with a uniform flow assumption as described by Manning's equation (eq. 6). A finite difference approximation of the kinematic wave model can be used to model watershed runoff on the surface and layer A.

$$\frac{\partial h}{\partial t} + \frac{\partial q}{\partial x} = r(x,t) \tag{5}$$

$$q = \alpha h^m \tag{6}$$

Where, *h*: water depth *m, q*: is discharge [m3/m.s], r is rainfall intensity [m/s], *t* is time [s], *x* is distance from the upstream edge, and *α, m* is constant concerning friction

4.4 Linear Storage Model

We used linear storage model (eq. 7 & 8) for groundwater modeling in layers B-D in each mesh, thus the ground water storage can be evaluated in the proposed model.

$$\frac{dS}{dt} = I - O \tag{7}$$

$$O = (k_1 + k_2) \cdot S \tag{8}$$

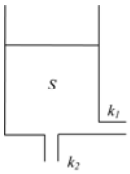

Where S: is storage amount [m], *I*: is inflow [ms^{-1}], *O*: is outflow [ms^{-1}], k_1, k_2: are coefficient of permeability

4.5 Initial and Transmission Losses Model

The SCS (Soil Conservation Service) method can be adopted to calculate initial losses in Wadi Assiut catchment. The method (SCS. 1985) has been successfully applied to ephemeral watersheds in SW US. Runoff in sub basins occurs after rainfall exceeds an initial abstraction (Ia) value. Rainfall excess, Q, in NRCS method is related to the effective potential retention value, S, as given in eq. 9.

$$P_e = \frac{(P - I_a)^2}{P - I_a + S} \tag{9}$$

The initial abstraction is suggested by SCS to be approximately 20 % of the maximum potential retention value. The initial abstraction consists mainly of interception, infiltration prior to runoff, and surface storage, and is related to potential maximum retention as given in eq. 10.

$$I_a = 0.2S \tag{10}$$

S (mm) is the maximum retention parameter as given in eq. 11.

$$S = \frac{25400 - 254CN}{CN} \tag{11}$$

Where, P_e = Accumulated precipitation excess at time t (mm), P = Accumulated rainfall depth at time t (mm), I_a = the initial loss (mm), S = potential maximum retention (mm)

The catchment's capability for rainfall abstraction is inversely proportional to the runoff curve number. For CN = 100, no abstraction is possible, with runoff being equal to total rainfall. On the other hand, for CN = 1 practically all rainfall would be abstracted, with runoff being reduced to zero. The curve number CN value depends on hydrologic soil group and land use cover complex. The hydrologic soil groups are defined by SCS soil scientists as A, B, C, and D are classified based o the soil type and infiltration rate. So, based on the land use, soil type and infiltration rate, the curve number of the land use in the studied area can be estimated.

Transmission losses are important not only in their obvious effect on stage flow reduction, but also as a source of ground water recharge to underlying alluvial aquifers. The variables that are considered useful in estimating the variation in the transmission loss included; 1-the flow volume at the upstream end of the reach, 2-channel antecedent condition, 3-chaneel slope, 4- channel bed material, the duration of the flow, 5- channel width. Walter's (1990) developed an equation to calculate the transmission losses as given in Eq. 12.

$$V_1 = 0.0006225 W^{1.216} V_A^{0.507} \tag{12}$$

Where V_1 =transmission loss for the first mile (acre-ft), V_A = upstream flow volume (acre-ft), w=active channel width. The distributed transmission losses can be calculated in the Wadi system using this equation.

5. Results and Application

Hydro-BEAM is a multilayer hydrological model, four layers (A-D); A-Layer is composed of the surface and soil surface layer. kinematic wave model and Manning eq. are used to estimate the surface runoff and roughness coefficient in each mesh. B-D-Layers (subsurface) are evaluated using linear storage model. The flow in each of B and C layers is flowing toward the river, but D-layer is considered as groundwater storage. When storage water content reaches to thickness and becomes saturated state, water content flows into the upper layer of model as returned style. It consists mainly of three main modeling parts; climatic modeling, watershed modeling and the main program modeling. The simulation period is from 1994 to 1995 based on geographical and climatic data where Egypt subjected to a big rainfall event on November 1994. The watershed modeling of Wadi Assiut is achieved based on DEM data by using GIS. The digital topological map of Wadi Assiut is demonstrated as shown in Figure 4A. It is clear that the general slope from NE corner to SW corner.

Land use types can be reclassified from the data of GLCC. The model result of land use distribution can be depicted as mountains, field, desert, city, and water as demonstrated in Figures 4B, 4C, 4D, 4E and 4F respectively. From the distribution maps of land use, it was found that the mountains and forest are limited, and the agricultural field is concentrated at

the Southwestern part. Desert is the majority of land use types. The distribution of urban and water are concentrating at the south western side of Wadi Assiut.

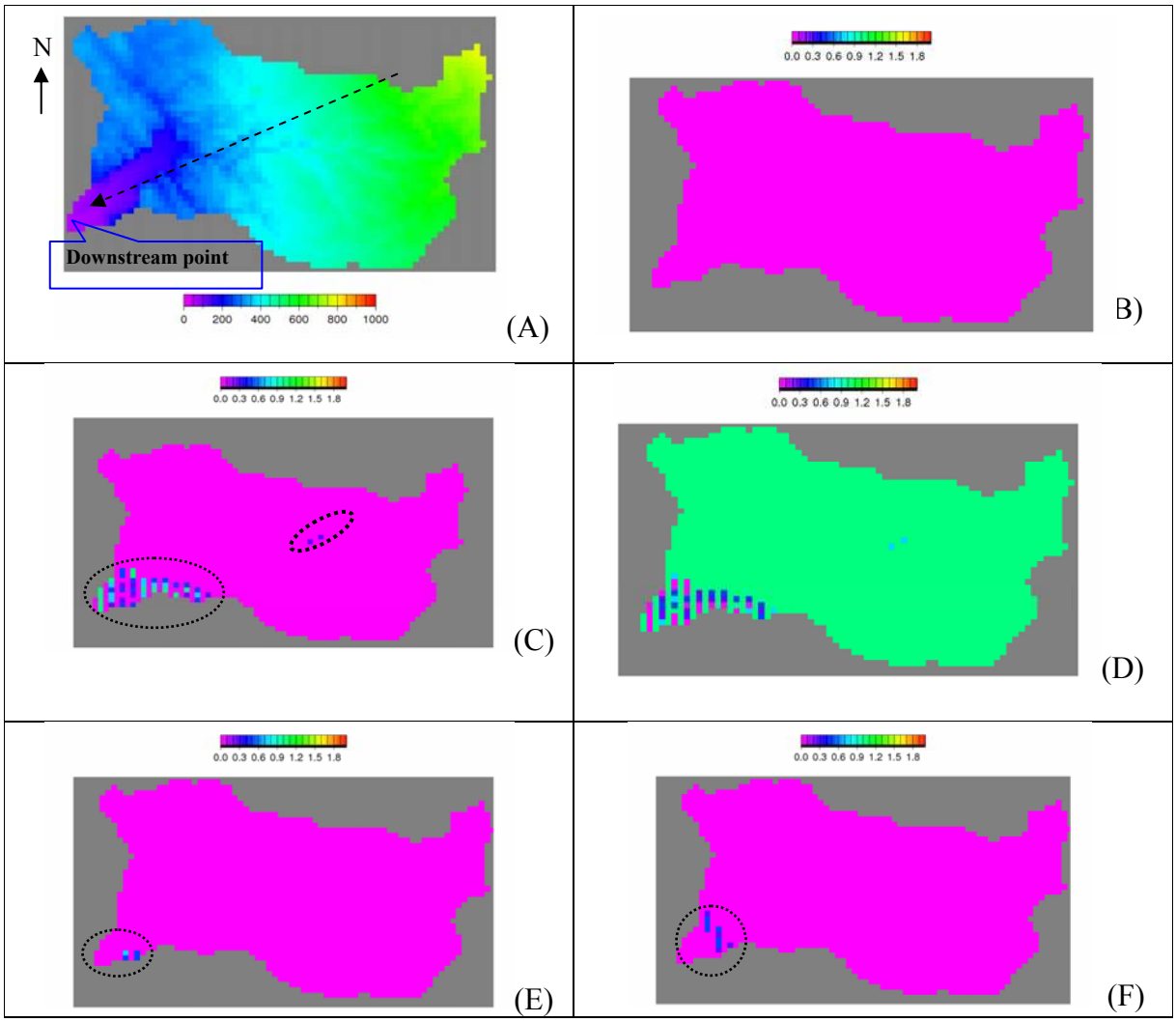

Figure 4 Modeled topographical map of Wadi Assiut watershed (A), distribution map of mountains (B), distribution map of filed and paddy field (C), distribution map of desert (D), distribution map of city (E), and distribution map of water (F).

The surface flow discharge can be demonstrated in Wadi Assiut watershed using the climatic data of the two years (1994-1995), where the daily and hourly output results can be obtained using Hydro-BEAM. However the lack of observed data, the simulated results are reasonable and satisfied due to good agreement between discharge hydrograph and rainfall hyetograph as shown in Figure 5A. The maximum peak of the runoff in Wadi assiut is 85m3/s and the rainfall maximum peak is about 12.7mm/hr.

The simulation of hourly discharge also is accomplished as the maximum peak of is 49 m3/s as shown in Figure 5B. The results of daily and hourly simulations (simulation period is November 2-5, 1995) are completely coincide in their curve shape, thus the behaviors of the Wadi system can be declared using the proposed model.

From the distribution map of surface runoff, we noticed that the discontinuous flow is perfectly depicted as shown in Figure 6A, so the most import characteristics (the discontinuous surface flow) in the ephemeral streams is successfully evaluated.

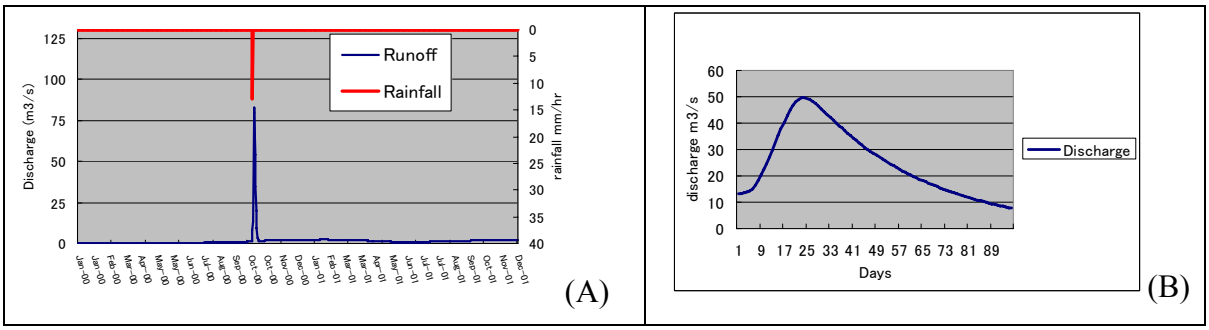

Figure 5 Daily discharge simulation hydrograph and rainfall hyetograph (A), Hydrograph of hourly discharge simulation (B)

The merit of our model is evaluation the interaction between surface and subsurface water due to its importance in the arid regions. So, based on the linear storage model, the equivalent ground water storage can be investigated.

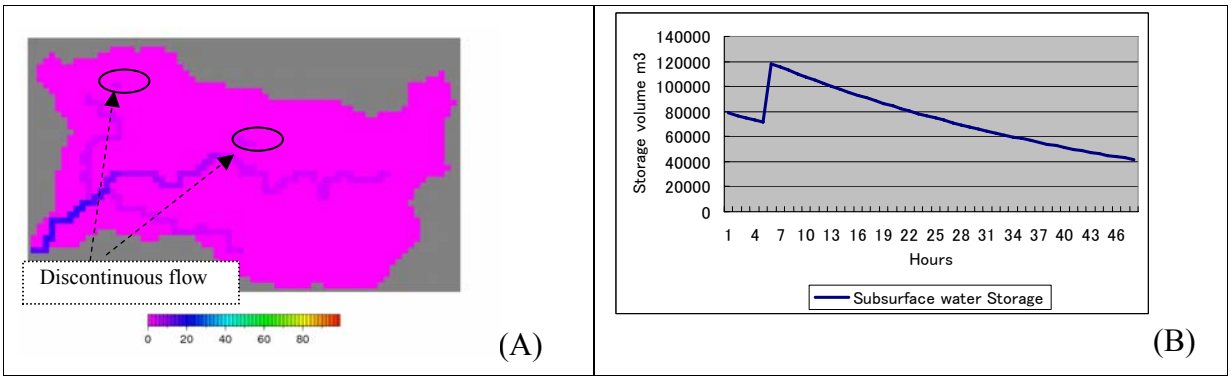

Figure 6 Distributed map showing the discontinuously surface flow (A), hydrograph of subsurface water equivalent storage (B)

It is declared that the subsurface water storage is affected by the flood where the hydrograph of subsurface water storage increased during flood event and then gradually decreased during the recession of the flood as depicted in Figure 6B.

Quantification of transmission loss is important, but it raises a number of difficulties. Walters (1990) provided evidence that the rate of loss is linearly related to the volume of surface discharge. They are evaluated by using Walter's equation and the balance method (the difference between inflow and out flow in each mesh). A good agreement between the results of transmission losses using the two methods is found as shown in Figure 7A. The maximum peak of transmission losses is 13m3/s by using Walter's method and 15m3/s by using balance method. It is deduced that the transmission losses contribute to the ground water as the main recharge for the subsurface water in the Wadi system. We noticed that the linear relationship between the transmission losses and discharge hydrographs as shown in Figure 7B, Moreover, you can see that the transmission losses curve at the recession of the flood is approximately equal to runoff.

Because of our main targets in this research are water resources management and flood control, the conjunctive use of surface and subsurface water can be used for the real application. A lot of surface water infiltrated as the main resource of recharge to the subsurface due to the transmission losses. This subsurface water can be utilized for domestic and agriculture use.

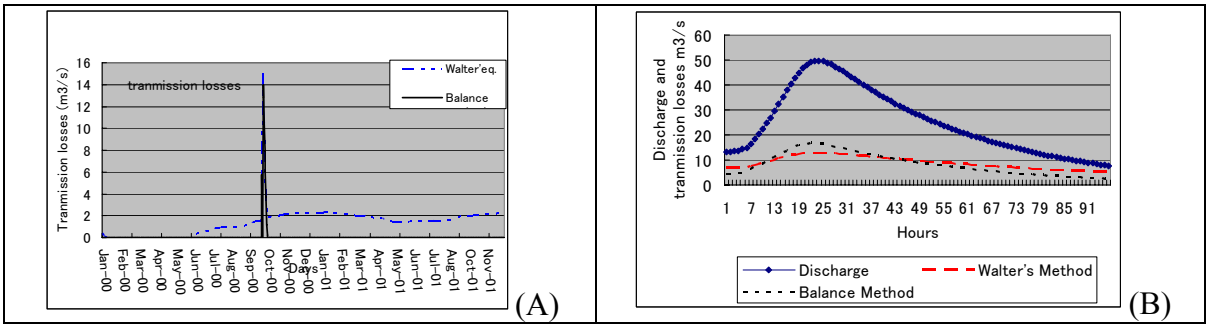

Figure 7 Transmission losses simulation (Walter's Eq. and Balance method) (A), comparing of discharge and transmission losses (Walter's Eq. and Balance method) (B)

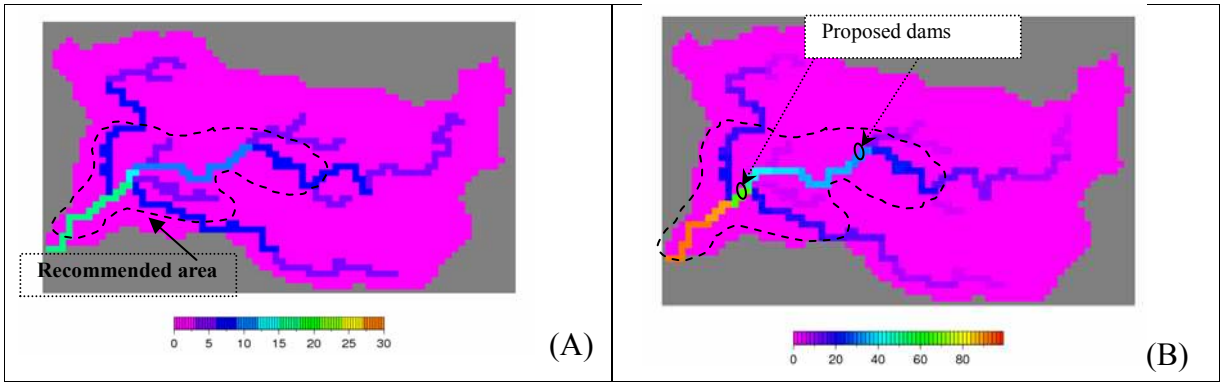

Figure 8 Distribution map of transmission losses (A), distributed map showing the maximum surface runoff (B)

Constructing the pumping wells in the middle and western parts of Wadi Assiut is recommended as declared in Figure 8A. The surface water during the flood event or the rainy season can be used for the agriculture purposes. We propose for the flood control and water resources management to establish two dams along the main channel of Wadi Assiut due to the maximum discharge during the flood at the two locations as shown in Figure 8B. They will be useful for protection the people from any flood threat and to increase the recharge to the subsurface water which can be used for the long term for people needs.

6. Conclusion

Hydro-BEAM has been chosen as distributed model for the Wadi System modeling. Modifications of Hydro-BEAM have been made to simulate the surface runoff in the ephemeral streams and to estimate the transmission losses which are the main source of the recharge to subsurface water. The runoff simulation is successfully achieved in the Wadi system. The maximum peak of the runoff in Wadi Assiut is 85m^3/s for the simulation period from (1994-1995). The rainfall maximum peak is about 12.7mm/hr. The simulation of hourly discharge also is accomplished where the maximum peak of discharge is 49 m3/s, the simulation period is November 2-5, 1994. The behaviors of the Wadi system can be declared using the proposed model as depicted in our simulation.

The transmission losses can be evaluated using two methods; Walter's eq. and the balance method and the results are reasonable due to their agreement. It is concluded that

transmission losses participate as the main source of recharge to the subsurface. It is noticed that it is affected by the volume of surface runoff as evidence that the rate of losses is linearly related to the volume of surface discharge.

The novelty of this research is that the proposed model shows the discontinuously surface flow of the Wadi system, in addition to the distribution of the equivalent subsurface water storage. The conjunctive use of surface and subsurface water can be used in the real application for flood control and water resources management in Wadi Assiut. It is recommended that the western and the middle parts of Wadi Assiut can be utilized for pumping of subsurface water and establishment the dams to protect the people from the flood thread and increase the water resources to overcome the problem of the water shortage.

It is concluded that the proposed model is considered an applicable methodology in larger areas and consequently, a vital contribution to estimate the distributed surface discharge and equivalent of subsurface water storage regionally not only in Wadi Assiut, Egypt but also in other arid regions. Much more researches are recommended for the Wadi system modeling based on the observed data. The regional application of the Wadi system model is our future target.

REFERENCES

Andersen, N.J., Wheater, H.S., Timmis, A.J.H. and Gaongalelwe, D. (1998), Sustainable development of alluvial groundwater in sand rivers of Botswana. In *Sustainability of Water Resources under Increasing Uncertainty, IAHS* Pubn. No. 240, pp 367-376.

Goodrich, D.C., Lane, L.J., Shillito, R.M., Miller, S.N., Syed, K.H. and Woolhiser, D.A. (1997), Linearity of basin response as a function of scale in a semi-arid watershed. *Water Resour. Res.*, 33,12, 2951-2965.

Hamaguci, T., Kojiri, T. and Saber, M. (2007), Hydrological application of upscaling technique based on homogenization theory, *Proceeding of 2007 Annual Conference, Japan Socity of Hydrology and Water Resources*, pp. 44-45.

Knighton AD, Nanson GC. (1997), Distinctiveness, diversity and uniqueness in arid zone river systems. In Arid Zone Geomorphology: *Process, form and Change in Drylands (2nd edn), Thomas DSG (ed.). John Wiley & Sons: Chichester*; pp. 185–203.

Kojiri, T., Tokai, A., and Kinai, Y. (1998), Assessment of river basin environment through simulation with water quality and quantity. *Annuals of Disaster Prevention Research Institute,* Kyoto University, No. 41 B-2, pp. 119-134 (in Japanese).

SCS (1985), National Engineering Handbook, section 4: *hydrology, US Department of Agriculture, Soil Conservation Service, Engineering Division, Washington, DC*.

Sorman, A.U. and Abdulrazzak, M.J. (1993), Infiltration - recharge through Wadi beds in arid regions. *Hydr. Sci. Jnl.*, 38, 3, 173-186.

Stephens, D.B. (1996), Vadose zone hydrology. *CRC Press–Lewis Publishers, Boca Raton*

Telvari, A., Cordery, I. and Pilgrim, D.H. (1998), Relations between transmission losses and bed alluvium in an Australian arid zone stream. *In Hydrology in a Changing Environment. Eds Howard Wheater and Celia Kirby,Wiley*, Vol II, pp 361-36

Walters, M.O. (1990), Transmission losses in arid region. *J. of Hydraulic Engineering*, 116, pp. 127-138.

Wheater, H.S., Woods Ballard, B. and Jolley, T.J., (1997), An integrated model of arid zone water resources: evaluation of rainfall-runoff simulation performance. In: Sustainability of Water Resources under Increasing Uncertainty, IAHS Pubn. No.24

NRCS CURVE NUMBER EMPLOYED HYDROLOGIC HOMOGENEOUS REGIONALIZATION IN REGIONAL FLOOD FREQUENCY ANALYSIS

Binaya Kumar Mishra[1], Kaoru Takara[2] and Yasuto Tachikawa[3]

[1] Graduate Student, Department of Urban and Environmental Engineering, Kyoto University
Uji Campus, Kyoto, 611-0011, Japan, e-mail: mishra@flood.dpri.kyoto-u.ac.jp
[2] Professor, Disaster Prevention Research Institute, Kyoto University
Uji Campus, Kyoto, 611-0011, Japan, e-mail: takara@flood.dpri.kyoto-u.ac.jp
[3]Associate Professor, Department of Urban and Environmental Engineering, Kyoto University
Katsura Campus, Kyoto, 615-8540, Japan, e-mail: tachikawa@mbox.kudpc.kyoto-u.ac.jp

ABSTRACT

Estimation of extreme flood for different return period is required in design of various hydraulic structures. Regional flood frequency analysis is an effective method for estimating such extreme flood. Delineation of hydrologic homogeneous regions is key step in success of regional flood frequency analysis. This study deals hydrologic regionalization of Nepalese territory. Cluster analysis, a multivariate technique, is generally used to identify objectively hydrological regions. This work addresses the difficulty of allocating suitable weight to different clustering attributes by employing NRCS runoff curve number. On superimposing monsoon rainfall pattern map over runoff curve number map, five hydrologic regions were proposed. L-moment based regional hydrologic homogeneity test led finalization of hydrological homogeneous regions.

Keywords: curve number, flood frequency, homogeneity test, L-moment

1. INTRODUCTION

Estimation of extreme flood for different return periods is required in design and planning of various water related structures. This extreme flood is popularly known as design flood. Design flood estimation methods can be broadly classified into two groups: streamflow-based methods and rainfall-based methods. This work is related to streamflow-based methods which base their analysis purely on stream-gauging data. The most common streamflow-based methods are the flood frequency analysis and regional flood frequency analysis. Flood frequency analysis is applicable to locations which possess long records of observed flood data. However, the gauged locations rarely coincide with the locations at which water-related structures are going to be constructed. In such situation, regional hydrological characteristics need to be used in estimation of design flood. Regional flood frequency analysis is such method which makes the use of regional hydrological characteristics for estimating design flood. Regional flood frequency analysis is popular method for estimating flood peaks within specified probabilities of exceedance at ungauged sites or enhancing estimation at gauged sites where historical records are short.

Among various methods (Cunnane, 1998) of regional flood frequency analysis, index flood method is the most popular. The index flood procedure includes three major steps: hydrologic homogeneous regionalization, selection of regional distribution function and estimation of index flood (scale factor). This study deals with the first step i.e. hydrologic homogeneous regionalization. Regionalization refers grouping of territory/basins having

similar flood generating mechanisms. In other word, all the sites in a hydrologic homogeneous region possess identical frequency distribution apart from a site-specific scale factor. Regionalization is required to affect the spatial transfer of hydrologic information.

There are no specific guidelines for identifying homogeneous regions. This is due to the complexity in understanding precisely the factors that have effect on the generation of floods. Several attempts have been made by different authors to identify hydrological homogeneous regions in different parts of the world. Earlier research work used subjective consideration on the attributes like location, topography of the basin in forming hydrologic homogeneous regions. More recent works used multivariate technique such as cluster analysis to identify objectively hydrologic homogeneous regions. The cluster analysis is based either on physiographic characteristics or on flood data characteristics. Burn and Goel (2000) used three physiographic characteristics: catchment area, length of the main stream and slope of the main stream in central Indian River basins. Regionalization using basin characteristics such as catchment area, rainfall and soil type was suggested as an attractive approach of regionalization by Wiltshire (1985). Mosley (1981) used clustering of flood statistics: specific flood (peak discharge generated by unit drainage area) and coefficient of variance (C_v) for delimitation of New Zealand river basins. Burn (1997) used seasonality statistic (average date of flood events) to avoid the dual use (region forming and homogeneity test) of statistics derived from flood magnitudes.

Research on regionalization of Nepalese rivers is extremely limited. McDonald and Partners (1990) divided Nepalese territory into 7 regions using information for *low flow estimation*. Sharma and Adhikari (2004) has developed relationships for estimating extreme (minimum and maximum) and long-term (average) flows using regression technique by considering the whole Nepalese territory as one homogeneous region. Except similar previous work of Mishra et al. (2008), no other study is found on hydrologic regionalization of Nepalese rivers for design flood estimation. In the previous regionalization work, the authors used specific flood, date of flood events and lat-long of river basins as clustering attributes.

A number of difficulties were experienced by the authors in the earlier attempt. One of the major difficulties is different measuring units of clustering attributes. For example, one attribute like soil type is expressed in term of infiltration rate (mm/h) whereas another attribute like catchment area is expressed in km^2. Another problem is measuring scale (e.g., mm/hr or cm/hr) of clustering attributes. Because of different units/scale, a suitable weight needs to be allocated to each clustering attribute. Allocation of suitable weight to different clustering attributes is difficult and subjective work. A new approach of regionalization is presented here which addresses problems associated with different measuring units/scale of clustering attribute. Soil type, land cover, land slope and rainfall pattern are considered major physio-climatic attributes which govern flood generation. Effect of soil type, land slope and land cover can be taken into account by using NRCS runoff curve number (CN).

The present work identifies hydrologic homogeneous regions inside Nepalese territory. The work started with the estimation of runoff curve number for different combinations of soil type, land cover and land slope ranges. In next step, area-weighted CN was computed for spatially well-representing sample basins. These sample basins with drainage area smaller than 250 km^2 were generated from GTOPO30 digital elevation model (DEM). Hydrological regions were proposed by superimposing digitized monsoon rainfall map over CN associated basins map. Validation of proposed regions was made using the L-moment based regional homogeneity test. Theoretical background on NRCS runoff curve number and regional homogeneity test has been discussed in section 2 and 3 respectively. The following section deals study area, data analysis and region forming process. Results of the work and discussion on the obtained results have been discussed in section 7. The final section summarizes and concludes the present work.

2. NRCS RUNOFF CURVE NUMBER

The runoff curve number (CN), an index developed by USDA Natural Resource Conservation Service (NRCS), represents potential for storm water runoff within a drainage area. USDA developed runoff curve number from field experiments in small catchments for different combinations of hydrological soil group, land cover and soil moisture. Further research in different part of the world suggested adjustments in CN for different range of land slope and others. The curve number varies from 0 to 100; lower numbers indicate low runoff potential while larger numbers indicate increasing runoff potential. The CN is widely used for estimating direct runoff from a rainfall event. The runoff equation (Ritzema, 1994) is;

$$Q = \frac{(P - I_a)^2}{P - I_a + S} \tag{1}$$

where Q is direct runoff (mm), P is rainfall (mm), S is potential maximum retention (mm), and I_a is initial abstraction (mm). I_a is usually taken 20% of S. The runoff curve number, CN, is then related to S as:

$$CN = \frac{25400}{254 + S} \tag{2}$$

For NRCS runoff curve number estimation, the available soil data needs to be expressed into hydrological soil group. There are four hydrologic soil groups: A, B, C and D. These soil groups are roughly indicate high, moderate, slow and very slow infiltration rates respectively. The land cover is defined like woodland, forest, cropland, urban area etc. in estimating runoff curve number.

Soil moisture condition in the drainage basin before runoff occurs is another important factor influencing the CN value. Antecedent moisture condition (AMC) is based on the 5-day antecedent rainfall i.e. the accumulated total rainfall preceding the runoff under consideration. AMC I, II and III roughly indicate dry, average and saturated condition of drainage basins.

A curve number value based on different combination of hydrological soil group, land cover, land treatment, impervious percentage and land slope is available in tabular form. This table is popularly known as look-up table. Initially the look-up table is available for average moisture condition (AMC II). Then, if necessary, these CN values are modified based on 5-day antecedent rainfall data.

3. REGIONAL HOMOGENEITY TEST

Regional hydrologic homogeneity test is required for each proposed hydrologic regions. The L-moment based regional homogeneity test (Hosking and Wallis, 1997) needs computation of L-moment ratios: L-coefficient of variance (LC_v), L-skewness (LC_s) and L-kurtosis (LC_k) at each station for the available data series. Visually, regional homogeneity can be identified from the plot of LC_v *versus* LC_s or LC_s *versus* LC_k on L-moment ratio diagram (Rao and Hamed, 1997). If the plotted points are closer, the region can be expected as hydrological homogeneous. Numerically, there are two ways to check regional homogeneity. The first one is discordancy measure, intended to identify those sites that are unusual with the

group as a whole. The discordancy measure estimates how far a given site is from the centre of the group. If $u_i=[t^{(i)} \quad t_3^{(i)} \quad t_4^{(i)}]^T$ is L-moment ratios vector for the site *i* and superscript *T* as transpose of the vector, then discordancy (D_i) can be expressed as Eq. (3).

$$D_i = \frac{1}{3}(u_i - \bar{u})^T A^{-1}(u_i - \bar{u}) \tag{3}$$

where $\bar{u}$ and A in a region for N gauge locations are defined as;

$$\bar{u} = \frac{1}{N}\sum_{i=1}^{N} u_i \tag{4}$$

$$A = \sum_{i}^{N} (u_i - \bar{u})(u_i - \bar{u})^T \tag{5}$$

A site *i* is declared to be discordant if D_i is large. Critical value of D_i is 3 for the region having 15 or more nos. of gauged sites. For the region with smaller nos. of gauge sites, critical value of D_i varies with nos. of gauge sites in the region.

The second regional homogeneity test is heterogeneity measure, intended to estimate the degree of heterogeneity in a group of sites and to assess whether they might be reasonably treated as homogeneous. This test compares the variability of L-moment ratios for the catchments in a region with the expected variability obtained from simulation. The heterogeneity measure is expressed as:

$$H = \frac{(V - \mu_v)}{\sigma_v} \tag{6}$$

where V is the weighted variance of the LC_v or LC_s or LC_k for the region, μ_v is mean and σ_v standard deviation of V obtained from simulation. Heterogeneity measure H_1, H_2 and H_3 indicates variability in LC_v, LC_s and LC_k respectively. Heterogeneity measure H_1 is suggested as the most reliable parameter for testing regional homogeneity. A region is considered homogeneous if H<1, possibly heterogeneous if $1 \leq H < 2$, and definitely heterogeneous if $H \geq 2$.

4. STUDY AREA

This study is intended to form hydrologic regions inside the Nepalese territory for carrying regional flood frequency analysis. Nepal, roughly a rectangle in shape with an area of 147,181 square kilometer, is situated between China in north and India in remaining three sides. It has a length of 885 km east–west and width of 145–248 km north–south. Within this relatively small latitudinal extent, altitude rises from 60 m in south to the 8848 m (Mount Everest, the world's highest peak) in North. Physiographically, the country is divided into five regions (Figure 1): Terai (Plain), Siwalik Hills, Middle Mountains, High Mountains and High Himalayas.

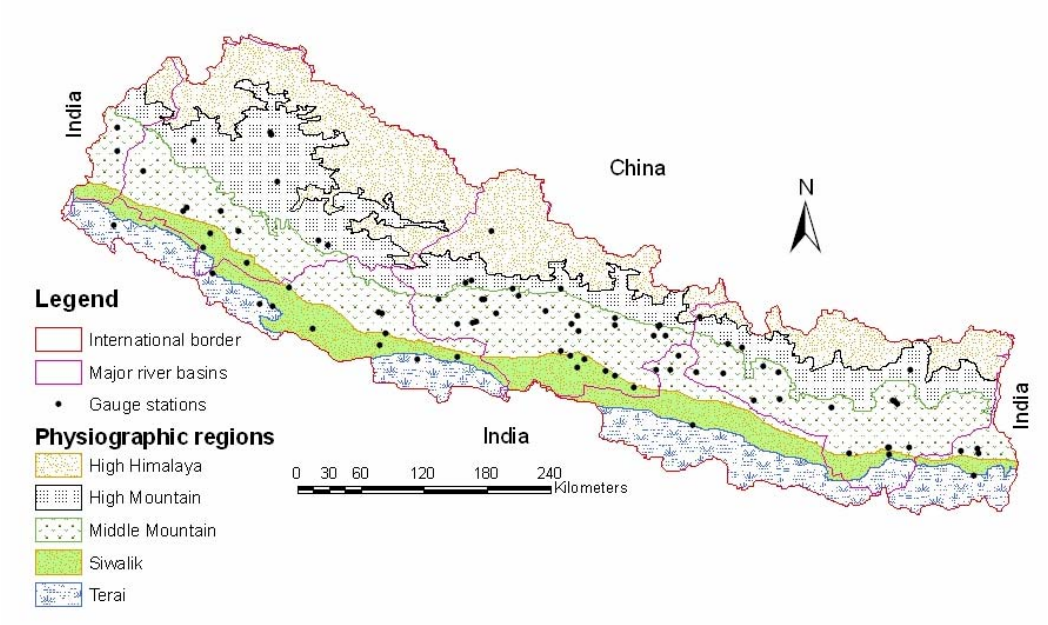

Figure 1 Physiographic regions of Nepal.

The average annual precipitation is around 1600 mm of which almost 80% or more occurs during the period of June-September. All the river systems of Nepal are tributaries to the Ganges river draining ultimately to the Bay of Bengal. The major tributaries generally flow towards south direction.

5. DATA AND PRELIMINARY ANALYSIS

The physiographic/climatic attributes: soil type, land cover, land slope and monsoon rainfall pattern have been considered in proposing hydrologic regions. Effect of soil type, land cover and land slope has been dealt using runoff curve number (CN). GTOPO30 digital elevation model (DEM) was used in generating sample basins for the study purpose. Area-weighted runoff curve number value was calculated for each spatially representing sample basins. Annual instantaneous flood data of 49 river basins have been used for regional homogeneity test. Discussion on these data used is dealt in the following subsections.

5.1 Soil type

Global soil data at resolution of 5 arc-min (approx. 10 km) has been prepared by FAO and can be freely downloaded through internet. This digital soil map is available in shape file format with geographic coordinate system. Digital soil data of the study area was extracted from the downloaded large data set. Textural classification associated with soil data was considered important here since it can be easily converted into hydrological soil group which is required in CN estimation. Textural classes reflect the relative proportions of clay (fraction less than 0.002mm), silt (0.002 - 0.05mm) and sand (0.05 - 2mm) in the soil. Based on their proportion, hydrological soil group map of Nepal (Fig.2) was prepared.

5.2 Land cover

The University of Maryland, Department of Geography generated global land cover

classification collection in 1998. The university made fourteen land cover categories from the analysis of AVHRR satellites imagery acquired between 1981 and 1994. This land cover data can be freely downloaded at various resolutions through internet. Land cover data of the study area at resolution of 1km was made available from the internet site maintained by Global Land Cover Facility (GLCF). Digital land cover map (Figure 3) required for CN estimation purpose was prepared after simple modification in original classification.

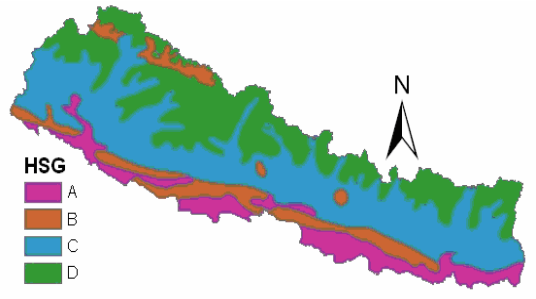

Figure 2 Hydrological soil groups of Nepal.

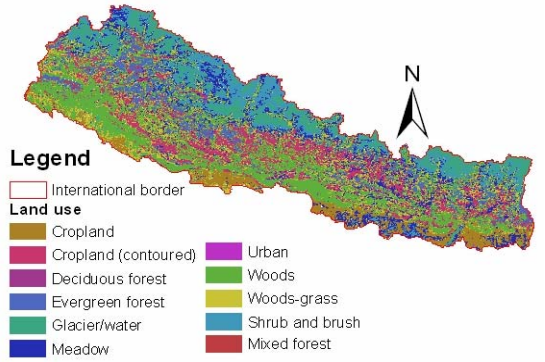

Figure 3 Land cover map of Nepal.

5.3 Rainfall distribution

Rainfall pattern i.e. distribution of rainfall over time and space is important in hydrologic regionalization. In general, annual rainfall amount decreases slightly from east to west and increases with elevation from south to north on windward slopes. Monsoon rainfall which occurs during the months of June to September has more importance in regionalization for design flood estimation. About 80 or more percent of the annual rainfall occurs during this season and the rainfall regime covers the whole country except the northern Himalayan region. Such concentration of rainfall during a few months results large floods and landslides. The study made three classes of monsoon rainfall pattern from mean monsoon precipitation map available at http://www.fao.org/ag/agL/swlwpnr/reports/y_sa/z_np/npmp134.htm . These classes (Figure 4) were defined for rainfall value less than 1000 mm, 1000 to 1500 mm and more than 1500 mm.

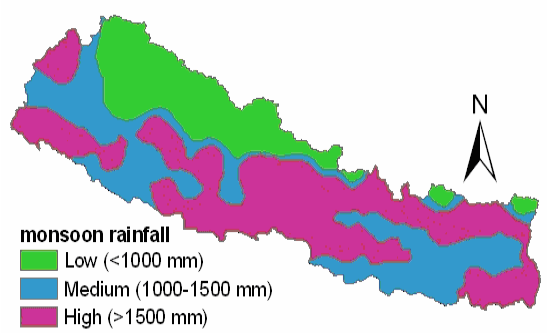

Figure 4 Monsoon rainfall map of Nepal.

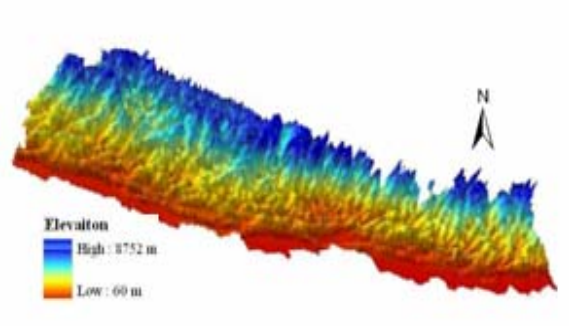

Figure 5 GTOPO30 DEM of Nepal.

5.4 Digital elevation model

Digital elevation model (DEM) of the study area (Figure 5) was clipped from large GTOPO30 DEM of Asia. This can be freely downloaded from the internet site maintained by

global data centre of NASA. This 30 arc-sec (approx. 1 km) resolution DEM was used to generate spatially representing sample basins and stream network using Arc GIS. The stream network derived from this DEM was compared with the stream network available in various reports available at internet and found acceptably okay. Also, the areas of river basins for the gauged outlets generated from DEM were compared with the areas made available by department of hydrology and meteorology (DHM), Nepal for further validation of downloaded DEM.

5.5 Flood data

Regional hydrologic homogeneity test need to be performed on each of the proposed hydrologic region. It needs adequate number of gauge station with long record length of flood data. Department of Hydrology and Meteorology (DHM), Nepal is one and only government organization responsible for collecting and distributing flood data in Nepal. Regularly observed instantaneous annual maximum stream flow data were collected for 49 stream gauging stations in Nepal. Selection of these stream gauging stations were based on basins' boundary position and record length of observed data. Boundaries of all these stations are restricted inside a proposed hydrologic region. Most of these stations are situated in middle mountain region. Out of these 49 considered river basins, 46 have observed length of more than 10 years. Because of inadequate gauging stations in lower region, 3 stations were selected though their record length is smaller.

Analysis of flood data was started by visual inspection. These flood data have been obtained from the 1998, 2003 and 2004's DHM publications. In addition, some recent flood data were collected in digital format from the authority of DHM, Nepal. In case of overlapping mismatched data, the latest publication was considered as correct flood data. The flood data series being homogeneous and stationary are the basic assumptions in flood frequency analysis. Test of homogeneity and stationary for the flood data series was performed as discussed by Mann and Whitney (1947). All the data series were found homogeneous and stationary at 5% significance level. Presence of outliers in the data causes difficulties when fitting a distribution to the data. The G-B test (Grubbs and Beck, 1972, Rao and Hamed, 2000) was used to detect outlier. Approximate relationship proposed at 10% significance level by Pilon and Harvey (1993) was used in calculating G-B statistic. The study found 1 no. of outliers at 14 stations (station indices: 267, 404.6, 438, 439.8, 445.3, 465, 530, 570, 589, 602, 620, 627.5, 650 & 660), 2 nos. at station index 447.9 and 3 nos. at station index 241.

6 REGION FORMING PROCESS

The region forming started with development of NRCS runoff curve number map for hydrological soil group, land cover and land slope. Since information on rainfall amount prior to the instantaneous flood data series could not be obtained, average soil moisture was considered while estimating the runoff curve number. Arc CN-runoff tool (Zhan and Huang, 2004), a rainfall-runoff model on Arc GIS platform, can generate efficiently runoff curve number map. The tool Arc CN-runoff requires with a look-up table (Table 1) consisting specific number between 0 and 100 for different soil type, land cover and land slope combination. Area-weighted average runoff curve number was calculated for each of 650 sample basins. The present study did not consider sample basins from Himalayan region considering its insignificance in monsoon flood. Hydrologic regions were proposed by superimposing monsoon rainfall map over sample basins associated with CN values.

Table 1 CN association with HSG and land cover.

Land cover	Soil Type			
	A	B	C	D
Meadow	30	58	71	78
Woods - Grass (Fair)	43	65	76	82
Woods (Fair)	36	60	73	79
Deciduous Forest	36	60	73	79
Evergreen Forest	40	66	77	85
Mixed Forest	38	63	75	82
Urban	68	80	88	94
Cropland	49	69	79	84
Cropland (terraced)	65	74	82	86
Shrub / Brush Tundra	48	67	77	83
Glaciers/Stream/Lake	0	0	0	0

The L-moment based regional hydrologic homogeneity test was applied on each proposed regions. To apply the homogeneity test, L-moments/ratios were computed for collected flood data at each station. Heterogeneity measure, particularly H_1, was checked for each region. The region for which heterogeneity measure was found smaller/nearer to 2 was accepted as homogeneous region. For the region having heterogeneity measure far beyond 2, discordancy measure (D_i) was taken into consideration to make adjustment in proposed regions. When heterogeneity measure and discordancy measure reduced to limiting value, the region was declared hydrological homogeneous.

7 RESULTS AND DISCUSSION

Out of total 650 sample basins, 450 nos. were found with CN varying from 73 to 80. The remaining basins were found with smaller curve number ranging from 50 to 65. This observation led 2 divisions of Nepalese territory. The basins with higher CN were found mostly in mid-mountain and higher mountain whereas sample basins with smaller CN values were found in low-mountain and plain region.

Monsoon rainfall map was superimposed over the proposed CN based regional map for further regionalization. Superimposition of monsoon rainfall map over CN-regional map led additional 3 hydrologic homogeneous regions. In this way, the study proposed total of 5 hydrologic regions and proceeded for validation of the regions.

For validation, hydrologic homogeneity test was performed in each region using historical flood data series. Heterogeneity measures H_1, H_2, H_3 before and after removing the discordant stations are given in Table 2. A value of H_1= 8.9 was found when considered all stations of Nepalese territory. The situation improved not much even after removing discordant sites. This value is far beyond the acceptable limit indicating hydrological non-homogeneity of Nepal. The regions 2, 3 and 5 were found with acceptable value of heterogeneity measure and with no discordant sites in first attempt. The value of H_1 was found as 5.72 and 4.77 for regions 1 and 4 respectively before removing the discordant sites. When discordant sites were removed and some adjustments were made in the proposed region, the heterogeneity measure reduced near acceptable limit for region 1 and region 4. Figure 6 shows the finally identified 5 nos. of hydrologic homogeneous regions.

Table 2 Regional heterogeneity measures for Nepalese river basins.

Region	% area	All				Discordant sites removed			
		Nos. of sites (NS)	H_1	H_2	H_3	NS	H_1	H_2	H_3
All	100	49	8.9	2.53	-0.45	44	6.36	1	-1.67
1	16.24	9	5.72	1.41	-0.44	7	1.13	-0.07	0.11
2	14.67	2	-0.41	-0.7	-0.62	2	-0.41	-0.7	-0.62
3	33.20	10	1.96	1.1	0.09	10	1.96	1.1	0.09
4	24.63	26	4.77	1.22	-0.14	24	2.09	0.08	-0.96
5	11.26	2	-1.08	0.69	0.01	2	-1.08	0.69	0.01

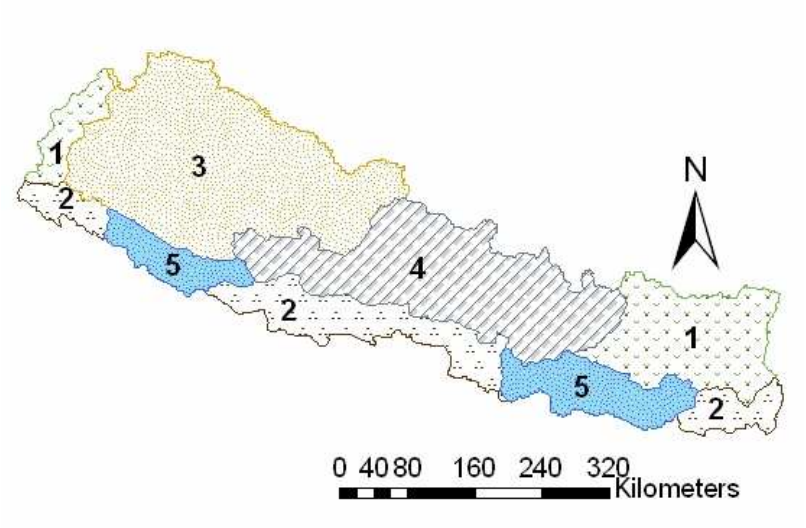

Figure 6 Hydrological homogeneous regions of Nepal.

8 SUMMARY AND CONCLUSIONS

Difficulties associated with mostly used regionalization technique i.e. clustering technique were discussed. Use of runoff curve number (CN) was proposed to address difficulties like attributes' measuring units/scale and suitable weight in cluster analysis. To estimate the runoff curve number, land cover map prepared from AVHRR satellite imagery and soil data prepared by FAO were brought in use. Hydrologic regions were proposed by superimposing monsoon rainfall map over runoff curve number map. The L-moment based regional hydrologic homogeneity test led some adjustment in proposed regions and finally 5 hydrologic regions were identified inside the Nepalese territory.

The main objective to delineate hydrological homogeneous regions for flood frequency analysis was achieved despite the complexity in understanding precisely the factors that have effect on generation of floods. Heterogeneity measures for each region were found within or near critical values. This led to conclude the runoff curve number employed regionalization approach as effective approach of hydrologic regionalization. The present regionalization work will be able to predict design flood better as compared to the previous work. In the next stage, the authors will estimate regional distribution function and index flood for each delineated region to accomplish the regional flood frequency analysis. To justify this new approach of hydrologic regionalization, the approach will be applied in country/territory other than Nepal.

ACKNOWLEDGMENTS

We would like thank to MEXT, Japan for providing financial support in carrying research work. We would also like to thank Innovative Disaster Prevention Technology and Policy Research Lab, Kyoto University, Japan for funding/technical support.

REFERENCES

Burn, D.H. (1997): Catchment similarity for regional flood frequency analysis using seasonality measures, *Journal of Hydrology*, Vol. 202, pp. 212-230.

Burn, D.H. and Goel, N.K. (2000): The formation of groups for regional flood frequency analysis, *Hydrological Sciences Journal*, Vol. 45, No. 1, pp. 97-112.

Cunnane, C. (1998): Methods and merits of regional flood frequency analysis, *Journal of Hydrology*, Vol. 100, pp. 269-290.

Grubbs, F. and Beck, G. (1972): Extension of sample sizes and percentage points for significance tests of outlying observations, *Technometrics*, Vol. 14, No. 4, pp. 847-854.

Hosking, J.R.M. and Wallis, J.R. (1997): *Regional Frequency Analysis: An approach based on L-moments*, Cambridge University Press, Cambridge, UK.

Mann, H.B. and Whitney, D.R. (1947): On a test of whether one of two random variables is stochastically larger than the other, *The annuals of mathematical statistics*, Vol. 18, pp. 50-60.

McDonald, M. and Partners Ltd (1990): *Hydrology and Agro-metrology Manual, M3, Design Manuals for Irrigation Projects in Nepal*.

Mishra, B.K., Takara, K. and Tachikawa, Y (2008): Regionalization of Nepalese river basins for flood frequency analysis, *Annual Journal of Hydraulic Engineering*, *JSCE*, Vo. 52, pp. 91-96.

Mosley, M.P. (1981): Delimitation of New Zealand Hydrologic Regions, *Journal of Hydrology*, Vol. 49, pp. 173-192.

Pilon, P.J. and Harvey, K.D. (1993): *Consolidated frequency analysis*, *version 3.1*, *reference manual*, Ecosystem Services and Evaluation Directorate, Environment Canada.

Rao, A. R. and Hamed, K.H. (2000): *Flood Frequency Analysis*, CRC Press LLC, Florida.

Rao, A.R. and Hamed, K.H. (1997): Regional frequency analysis of Wabash river flood data by L-moments, *Journal of hydrologic engineering*, Vol. 2, No. 4, pp 169-179.

Ritzema, H.P. (Editor-in-chief) (1994): *Drainage principles and applications*, International Institute for Land Reclamation and Improvement, Wageningen, The Netherlands.

Sharma, K.P. and Adhikari, N.R. (2004): *Hydrological Estimations in Nepal*, Kathmandu, Nepal.

Wiltshire, S.E. (1985): Grouping basins for regional flood frequency analysis, *Hydrological Sciences Journal*, Vol. 30, No. 1, pp. 151-159.

Zhan, X. and Huang, M. (2004): ArcCN-Runoff; an ArcGIS tool for generating Curve number and runoff maps, *Environmental Modelling and Software*, Vol. 19, No. 10, pp. 875-879.

CATCHMENT SCALE COMPARISON ON LUMPED REPRESENTATION FOR A DISTRIBUTED SEDIMENT RUNOFF MODEL

APIP [1], Yasuto TACHIKAWA[2], Takahiro SAYAMA[3], and Kaoru TAKARA[4]

[1]Student Member, Graduate Student, Dept. of Urban and Environmental Eng., Kyoto University
Kyoto 615-8540, Japan, e-mail: apip@flood.dpri.kyoto-u.ac.jp
[2]Dr. Eng., Associate Professor, Dept. of Urban and Environmental Eng., Kyoto University
Kyoto, 615-8540, Japan, e-mail: tachikawa@mbox.kudpc.kyoto-u.ac.jp
[3]Dr. Eng., Assistant Professor, DPRI, Kyoto University
Uji 611-0011, Japan, e-mail: sayama@flood.dpri.kyoto-u.ac.jp
[4]Dr. Eng., Professor, DPRI, Kyoto University
Uji 611-0011, Japan, e-mail: takara@mbox.kudpc.kyoto-u.ac.jp

ABSTRACT

This study analyses catchment scale effect to a lumped sediment runoff model performance derived from lumping a physically-based distributed sediment runoff model. The proposed lumped model takes into account the different sources of erosion and deposition processes on hillslopes. The eroded soils provided to river channel flow with sediment transport mechanism. To investigate catchment scale dependency of the new lumped sediment runoff model, sediment runoff simulations are conducted using different sizes of the catchment area and spatially averaged hourly rainfall. Four different sizes of catchment area are used, representing low-, medium-, and high- resolution. Then, the lumped model is installed for each catchment size scenario. The proposed method is examined by comparing water and sediment discharges simulated by the lumped and the original distributed sediment runoff models in the Lesti River basin, East Java, Indonesia.

Keywords: Lumping, catchment scale, sediment runoff model, Lesti River basin.

1. INTRODUCTION

The Lesti River catchment (381.2 km^2), a tributary catchment in the Upper Brantas River basin is selected as study area. The Brantas River, 320 km length with 39 tributaries and a catchment area about 11,800 km^2, is the second largest river located in East Java, has an average annual rainfall 2000 mm (80% fall in rainy season). At the confluence point of the Lesti River and the Brantas main reach, the Sengguruh dam was constructed in 1988 for water resources and power generation, which has the effect of trapping sediment into the Sutami Dam (formerly Karangkates) from the Brantas River and the Lesti River. The Sengguruh Dam has a catchment area of 1,659 km^2. Its original gross storage in 1989 was 22.4 million m^3 and reduced to 5.5 million m^3 in 1993. Unexpectedly, most of the gross storage has been already filled with the large amount of sedimentation from the Lesti River (Takara et al., 1996). The Lesti River transports sediment derived from the lahar (volcanic ashes and sands) of Mountain Semeru.

In order to effectively protect and manage water resources there is need to develop the science and to assemble the necessary information on which to base decision making. Herein, estimations of the changes in total runoff and sediment yield as well as an

understanding of those processes mechanism with time and space in the catchment scale are quite important for solution of a number of problems. Design and operational of dams and reservoirs, design of soil conservation, land-use planning, water quality and aquatic habitat management are some of the examples.

Mathematical models, including physically-based, can help to make quantified evaluation, prediction, or to understand the important processes and interactions in sediment runoff phenomenon. Physically-based distributed sediment runoff model and it lumping for Lesti River catchment were newly developed by authors (Apip et al., 2008 and Takara et al., 2001). The main propose to lump a distributed model is to produce a new lumped sediment runoff model version as interest in sediment runoff modelling extends to large catchments scale and to reduce computational time. Governing lumped model parameters derived physically by keeping the physical meanings of an original distributed model, which are obtained from integration of distributed equation according to lumping distributed approach and catchment characteristic from grid-cell based scale to the catchment scale, then new type of lumped model version is run without any additional calibration.

Earlier research results have shown that the rainfall runoff simulations from a well-validated hydrological model scale dependent to catchment area and the complex patterns. The lumped scale for rainfall runoff model is about 200 km^2, however the lumped scale of sediment runoff model is not clear. This paper illustrates the relation between catchment area, water discharge (total runoff), and sediment concentration by a combination of simulated of those values by an original distributed sediment runoff model and it lumped at different spatial scales inside study area.

2. DISTRIBUTED SEDIMENT RUNOFF MODEL

The physically-based distributed sediment runoff model has been developed to determine the runoff hydrograph, sedimentgraph, and total sediment runoff generated from any temporally-spatially varied rainfall event and continuous rainfall data input. The modeling approach is deterministic, physically-based, empirical, spatially distributed and dynamical in time. Dynamic spatial of water movements, erosion patterns and sediment rates can be predicted at any location inside the catchment as well. The concept of physically-based distributed sediment runoff modeling is shown in Figure 1. A sediment transport algorithm is newly added to the rainfall runoff model. Sediment runoff simulation can be divided in two parallel phases: runoff generation and soil detachment.

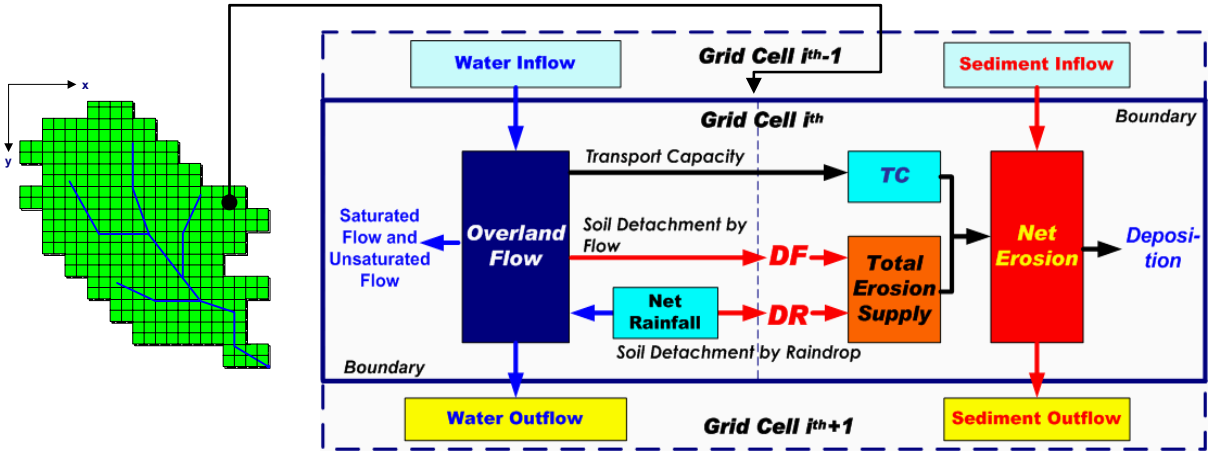

Figure 1 Schematic diagram of the physically-based distributed sediment runoff model within grid-cell scale.

For a given rainfall event, once the rainfall is directly added to subsurface or surface flow according to the water depth on the rainfall dropping grid-cell. The model does not consider the initial rainfall losses due to vertical water flow directly, such as infiltration effects. Rainfall runoff model effectively simulates lagged subsurface flow with calibrated hydraulic conductivities and soil layers depth.

The hydrological model considers three principal water flux pathways within a catchment: subsurface flow through unsaturated flow (capillary pore), subsurface flow through saturated flow (non-capillary pore), and surface overland flow. Using a stage-discharge relationship, after the water depth is greater than the surface soil layer, the net rainfall will accumulate as surface water and begin to flow as overland flow. Subsurface and surface flows in both land surface and river channel networks are computed as kinematic wave. The eroded sediment is transported by overland flow to river channels.

The sediment transport algorithm includes multiple sources of sediment transport, which are soil detachment by raindrop (*DR*) and hydraulic detachment or deposition driven by overland flow (*DF*). Soil detachment for interrill and rill implicitly are simulated respectively, rain splash and flow detachment. The erosion or deposition rates are calculated as a function of the hydraulic properties of the flow, the physical properties of the soil and the surface characteristic. The detachment of soil particles by raindrop impact is function of the energy imparted to the soil surface by the individual drops. The basic assumption of this model is that the sediment is transported and yielded when overland flow occurs. The transport capacity of the overland flow also needs to be specified, in which suspended sediment flow is calculated using the transport capacity approach, as it acts as an upper limit to the potential contribution of each grid-cell to sediment concentrations in saturated areas.

The simulation area is divided into an orthogonal matrix of square cells (250mx250m), assumed to represent homogenous conditions according to the digital elevation model (DEM). This allows the use of DEM to derive flow direction map to define the interaction between the objects which simulate sediment runoff at each grid-cell. Runoff generation, soil erosion or deposition are computed for each grid-cell and are routed between grid-cells using the kinematic wave model following water flow direction, which defines the routine order for the water flow and sediment transport propagation. The model uses the one-dimensional kinematic wave equation for both subsurface and surface flow.

3. LUMPING OF DISTRIBUTED SEDIMENT RUNOFF MODEL

Lumped Sediment Runoff Model Based on Traditional Method

A simple model of catchment response by separating hillslope process and river channel process (Sivapalan et al., 2002) is adopted and extended to incorporate sediment transport processes. This study uses the same principle to explore how sediment yield is related to hydrological response, erosion source, transport mechanism and depositional processes.

On a rainfall event basis, the sediment runoff processes are assumed only affected by surface runoff without consider the effect of sediment load from subsurface layer. According with storage-type concept, the model consists of three water stores, it called rainfall runoff model, and two sediment stores, it called sediment runoff model (Figure 2).

When the water depth larger than the maximum subsurface flow depth of Tank 1, surface runoff occurs and is added to Tank 2, outflow discharge (Q_w) from Tank 3 as a function of water storage amount (S_w) from each Tanks. After overland flow occurs, sediment transport mechanism on hillslope is computed (Tank 2). The sediment storage (S_s) in (Tank 2) is supplied by the balance between hillslope soil erosion rate, redeposition rate,

and sediment discharge released to river channel. Herein, soil erosion by effective rainfall (*DR*), soil erosion or redeposition by overland flow (*DF*) are calculated.

Similarly, at a given time *t*, the river channel store in Tank 3 is supplied with sediment material from the hillslope plus the river bed erosion, and only suspended bed material load is considered and soil detachment due to rain drop energy is negleted. Some of total sediment load, as amount of wash load plus suspended material load, in river channel store is redeposited back into river bed, while another fraction is transported to catchment outlet. Similarly with the hillslope process, the mass of sediment stored in the river channel is determined by the balance between hydraulic erosion rate, redeposition rate, and the release of sediment discharge to the catchment outlet. The rate of erosion or redeposition is depending on the transport capacity of flow and current sediment concentration carried by flow.

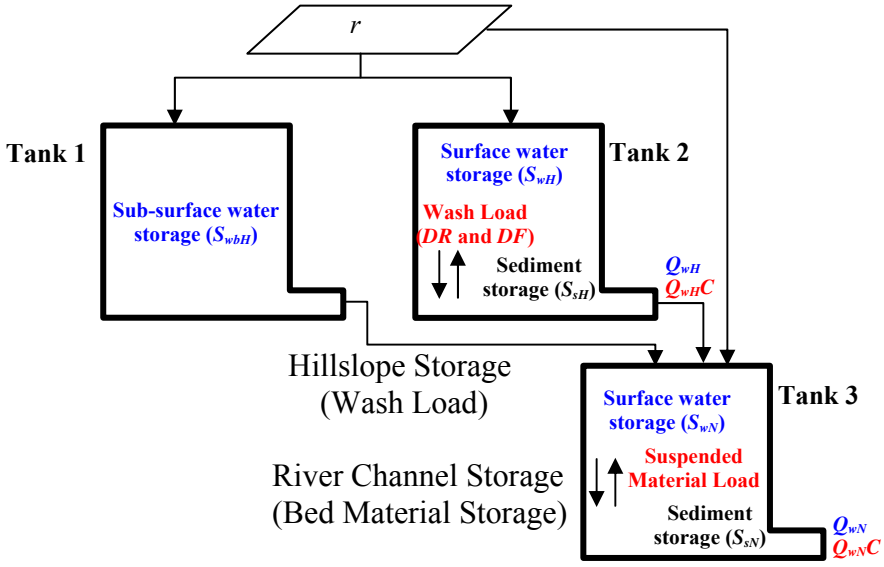

Fig. 2 Schematic diagram of the lumped sediment runoff model at catchment scale

The continuity equation of runoff and sediment models is represented as follows:
Hillslope process:

$$\frac{dS_{wH}}{dt} = r_H A_H - Q_H \tag{1}$$

$$\frac{dS_{sH}}{dt} = DR + DF_H - Q_H C_H \tag{2}$$

$$= k\,56.48\, r_H e^{-b*h_{s-avr}} + \left(\alpha \left(S_{sH}^{\max} - S_{sH}\right) h_{s-avr} - Q_H C_H 3600\right) / A_H$$

River channel process:

$$\frac{dS_{wN}}{dt} = r_N A_N + Q_H - Q_N \tag{3}$$

$$\frac{dS_{sN}}{dt} = Y_H + DF_N - Q_N C_N \tag{4}$$

$$= Q_H C_H + \left(\alpha \left(S_{sN}^{\max} - S_{sN}\right) h_{s-avr} - Q_N C_N 3600\right) / A_N$$

where k is the soil detachability (kg/J); KE is the total kinetic energy of the net rainfall (J/m^2); and b is an exponent to be tuned; $h_{s\text{-}avr}$ is the average of overland flow water depth at the

hillslope/river channel, Y_H is the hillslope sediment yield; α is the erosion/ deposition efficiency factor; r is the effective rainfall intensity; S_s^{max} is the maximum storage amount of sediment concentration; A is the total area; and the subscript of H and N show the hillslope and river channel section, respectively.

If the effective rainfall intensity is known, Eqs. (1,2,3,4) cannot be solved directly to obtain the outflow hydrograph and sedimentgraph from hillslopes or river channels, because other variables are unknown. A relationship is needed to relate Q, S_w, S_{ws}, $h_{s\text{-}avr}$, and S_s^{max} which are estimated from lumping distributed approach.

Lumping Distributed Rainfall Runoff Model

As first stage of lumped model development, a method to lump a distributed sediment runoff model for one layer, in case the sub-surface layer was assumed reached to saturated condition, was derived (Apip et al., 2007) as an extension from the lumping method proposed by Ichikawa et al., (2000). Herein, lumped rainfall runoff model derived from lumping distributed rainfall runoff model under steady-state condition is expressed by a non-linear reservoir, the storage is non-linearly related to outlet water discharge by storage constants K and p as follows:

$$S_w = K\,Q^p \tag{5}$$

by substituting Eq. 5 into Eq. 1 or Eq. 3 becomes:

$$\frac{dS_{wN}}{dt} = r_N\ A_N + Q_H - \left(\frac{S_w}{K}\right)^{1/p} \tag{6}$$

K is the model parameter having a physical meaning, can be interpreted as the time of concentration for a kinematic wave to travel across the system.

The value of K is derived from the lumping distributed rainfall runoff approach (Apip et al., 2007). K is influenced by spatially distributed of slope length (L), slope gradient (i), roughness coefficient (n), upper contributing area (U), and total area (A). It proves that K can be derived from the integration of distributed equation. In new lumped model, K is dimensional parameter ($m^{6/5}s^{3/5}$) is defined as:

$$K = \sum_{j=1}^{N} \frac{w}{(A)^p}\frac{k_j}{p+1}\left(\left(L_j + \frac{U_j}{w}\right)^{p+1} - \left(\frac{U_j}{w}\right)^{p+1}\right) \tag{7}$$

in which $p = \frac{1}{m}$, $k = \left(\frac{1}{\alpha}\right)^{\frac{1}{m}}$, and $\alpha = \frac{\sqrt{i}}{n} = \frac{\sqrt{\sin\theta}}{n}$

where i is the slope gradient (m/m), n is the roughness coefficient, m is the exponent constant, which can be shown to be 5/3 from manning's equation, and j is the number of grid-cell. Discharge per unit width (q), flow velocity (v), and water storage (s_w) for each grid-cell defined as:

$$q_i = \bar{r}\ \left(\frac{U_i}{w} + x_i\right),\quad h_i = \left(\frac{\bar{r}\left(\frac{U_i}{w} + x_i\right)}{\alpha_i}\right)^{1/m},\quad v_i = \left(\frac{Q}{A}\left(L_i + \frac{U_i}{w}\right)\right)^{1-p} k_i^{-1}$$

$$s_{wi} = w\left(\frac{\bar{r}}{\alpha_i}\right)^{1/m}\frac{1}{\frac{1}{m}+1}\left(\left(L_i + \frac{U_i}{w}\right)^{\frac{1}{m}+1} - \left(\frac{U_i}{w}\right)^{\frac{1}{m}+1}\right)$$

Total water storage at the hillslope area or river channel area are expressed as:

$$S_w = \sum_{i=1}^{N} s_{wi}$$

Lumping Distributed Sediment Runoff Model

The sediment runoff processes in this study are affected by dynamic spatial distribution of overland flow. The relationship between detachment and redeposition represented by Eq. 2 and Eq. 4 depends on the balance between S_s and S_s^{max}, the depth of overland flow or total runoff as well as. Those variables are produced from lumping distributed approach as:

The Maximum Sediment Storage (S_s^{max})

Many, mostly empirical, equations have been developed to predict sediment transport capacity of flow (*TC*) as function flow characteristics, slope, and material characteristics. These equations often use a threshold value of stream power, shear stress, or discharge. In this study, the transportation capacity is calculated based on the Unit Stream Power (USP) theory that can be applied for sediment transport in open channels and surface land erosion (Yang, 1973). The USP theory stems from a general concept in physics that the rate of energy dissipation used in transporting sediment materials should be related to the rate of material being transported. Sediment concentration in the water flow must be directly related to USP. The USP theory contributing to *TC* is defined as a product of the overland flow velocity, *v,* and slope, *i,* in the i^{th} grid-cell. Small particles such as clay and silt move mostly in suspension and easily carried by the flow while the sand fraction moves as bed-material and more difficult to move by flow. This is accomplished that *TC* depends on the particle settling velocity, shear velocity, grain size, kinematic viscosity of the water, and water density. A relationship between USP and the upper limit to the sediment concentration in the overland flow, C_t (ppm), can be derived (Yang, 1973 and Yang, 1979). Hence *TC* is the product of C_t as:

a. Surface Land and Erosion:

$$TC = \log C_t = I + J \log((vi - v_{critical} i)/\omega) \tag{8}$$

in which:

$$I = 5.435 - 0.386 \log(\omega D_{50}/NU) - 0.457 \log(U^*/\omega)$$

$$J = 1.799 - 0.409 \log(\omega D_{50}/NU) - 0.314 \log(U^*/\omega)$$

$$\omega = \sqrt{\frac{2}{3} + \frac{36}{\left(\frac{\rho_s}{\rho_w} - 1\right) g \left(\frac{D_{50}}{1000}\right)^{2/NU}}} - \sqrt{\frac{36}{\left(\frac{\rho_s}{\rho_w} - 1\right) g \left(\frac{D_{50}}{1000}\right)^{2/NU}}}$$

where vi is the unit stream power, m/s (v is flow velocity in m/s and i is the slope gradient m/m); $v_{critical}i$ is the critical unit stream power ($v_{critical}$ is the critical flow velocity); ω is the sediment fall velocity (m/s) calculated by Rubey's equation; ρ_s is the sediment particle density (kg/m^3); ρ_w is the water density (kg/m^3); g is the specific gravity (m/s^2); D_{50} is the median of grain size (mm); and NU is the kinematic viscosity of the water (m/s^2). $U^*(=\sqrt{g\,i\,h_s}\,)$ is the average shear velocity (m/s).

b. River Channel Erosion

The sediment transport function within river channel has been intended for the estimation of sediment transport rate or concentration at a nonequilibrium condition with deposition process. When the wash load and concentration of fine material is high, nonequilibrium bed-material sediment transport may occur, and its amount is a function of wash load. Wash load which depends on the supply from hillslopes has been assumed is high enough to significantly affect the fall velocity of sediment particles, flow viscosity, relative density of sediment and water.

For flow in river channel and at a nonequilibrium, transport capacity concentration of flow is modeled as a function of modified Yang's unit stream power, which is an expression for the total load with high concentration of fine sediment particle. Regarding Eq. 8 when sediment concentration is not too low, the incipient motion criteria, called critical stream power, can be neglected. To apply Eq. 8 to a river with a high concentration of fine materials and wash load, the values of viscosity, fall velocity, and relative density have to modified to consider the influence of high concentration of fine material on those values. Herein, the modified unit stream power formula proposed by Yang et al. (1979) is expressed:

$$TC = LogC_t = 5.165 - 0.153\frac{\omega_m D_{50}}{NU_m} - 0.297\log\frac{U_*}{\omega_m} + (1.780 - 0.360\log\frac{\omega_m D_{50}}{NU_m} - 0.480\log\frac{U_*}{\omega_m})\log(\frac{\gamma_m}{\gamma_s - \gamma_m}\frac{vi}{\omega_m}) \quad (9)$$

the coefficients in Eq. 9 are identical to those in Eq. 8. However, the values of ω, γ_s, and NU are modified for sediment transport in sediment-laden

The maximum sediment storage on hillslopes or river channels scale is defined as the total sediment transport capacity of overland flow in a whole of the hillslopes for each time step calculation. Therefore, we expressed the maximum sediment storage as the function of TC from the i^{th} grid-cell, surface water storage amount in the i^{th} grid-cell (s_{wsi}), and S_{ws}. The maximum sediment storage at hillslope area is calculated by adding up TC_i multiplied to s_{wsi} for all grid-cells as:

$$S_s^{\max} = \sum TC_i \; s_{w_i} / (S_w 1000) \quad (10)$$

TC (ppm) for the i^{th} grid-cell has been estimated by:

Sediment Concentration (C)

Based on the relationship between the current sediment storage (S_s) (kg/m^3/hr) and S_w for each time step calculation, the value of C from hillslope/river channel area can be solved:

$$C = \frac{S_s}{S_{ws}} \quad (11)$$

for each time-step calculation C is assumed to be uniform over the hillslope/river channel area and this is the variable of sediment continuity (see Eqs. 2 & 4).

4. COMPARISON OF LUMPED AND DISTRIBUTED MODEL UNDER DISCRETIZATION OF CATCHMENT AREA

The numerical experiments were run in two cases of rainfall event mode with hourly rainfall data input (Case 1: short duration, and Case 2: long duration) at four cases catchment

size. A digital topographic model for the Lesti River catchment was first developed and then four scenarios of the catchment size (Case A, Case B, Case C, and Case D), the high-, medium-, and low resolution of catchment size in term of lumped mechanism were delineated (see Figure 3) and it characteristics are given in Table 1. For each catchment size, average rainfall over whole area was used.

The original distributed sediment runoff model parameters were calibrated and validated using historical data for the 351.3 km^2 of the Lesti River catchment. These calibration and validation runs suggest that observed data of hydrological condition and sediment transport mechanism is generally amenable to the hydrological and sediment transport mechanism based on the original distributed sediment runoff model. The lumped model algorithm was applied to each synthetic of catchment area and compared with simulation results using distributed model.

Table 1 The characteristic of four cases catchment size in the Lesti River catchment

Catchment	Total grid-cell	Area (km^2)
Case A	404	25.3
Case B	1743	108.9
Case C	2114	132.1
Case D	6101	351.3

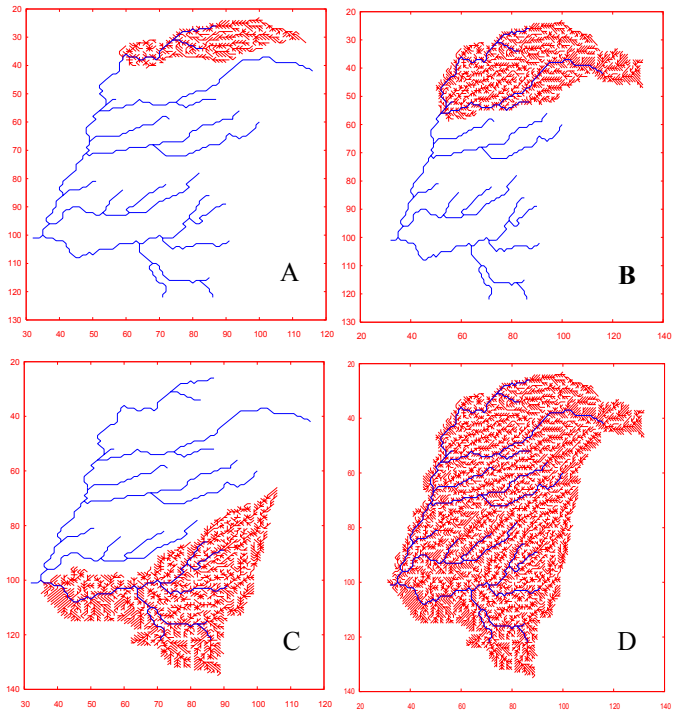

Figure 3 Lesti River catchment was partioned into four synthetic catchment area, in which red lines are the catchment area and blue lines are river channels.

Figure 4 is plots of the water discharge and sediment concentration by the physically-based distributed sediment runoff model and the lumped model for the entire period of rainfall scenario (Case 1 and Case 2). Figure 4 shows the discrepancy of simulation results between the original distributed model and it lumped model version for both water discharge and sediment concentration. The lumped model is in an acceptable way to reproduce the discharge and sediment concentration simulated by distributed model. All the values of correlation coefficient more than 0.90, its mean that the lumped model is in an acceptable way to reproducing the water discharge and sediment concentration calculated by distributed model. Just as with the case of sediment concentrations the correlation coefficients lower than outflow discharges.

However, in the case water discharge when the catchment size is increase, discrepancy between simulated values by the lumped and distributed models is generally higher. In the case of simulated sediment concentrations, the differences are higher than simulated water discharges, variation depending on the catchment size and characteristics as well as.

The discrepancy between lumped and distributed models for water discharges simulated in Case D under the rainfall condition Case 1 is higher than Case 2, in which the lumped model tends to underestimate, is due to the assumed steady state condition in deriving

lumped model, total rainfall in Case 1 is less than total rainfall of Case 2.

Conventionally sediment yield is held to decrease as basin area increases. For drainage areas in the range between small catchments and large basin (>10km^2), the effect of sediment sinks often becomes dominant over sediment sources, resulting in a gradual decline in sediment yield. The explanations for this is that large catchments often have more extensive floodplain development as well as footslopes where sediment are stored, the travel distance for sediment through catchment is longer and small catchments are more likely to respond directly to event driven flood than large catchments. The characteristics of sediment yield simulated by lumped model are consistent with these studies (see Case A).

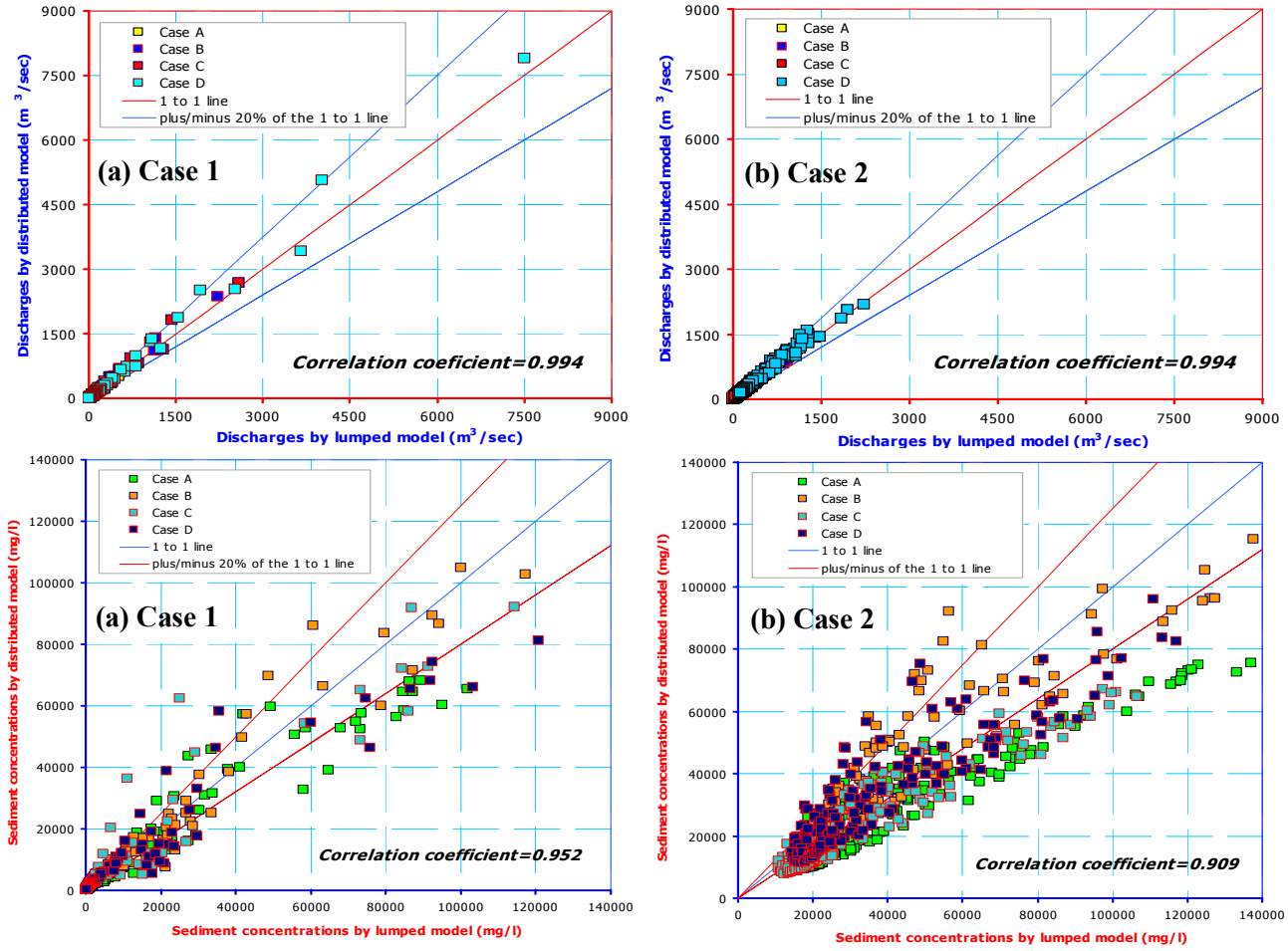

Figure 4 Comparison of simulated outflow discharges and sediment discharges by lumped and distributed models for two scenario rainfall data input: (a) Case 1; and (b) Case 2 and combined with four scenarios of synthetic catchment area.

CONCLUSIONS

Within the range of possible catchment area and soil depth, simulation results computed by the lumped model for hillslope area and river channel agree well with the simulation results computed by the original distributed model. For lumped rainfall runoff model, the discrepancy of the lumped model and distributed model increases when the catchment area and soil thicknesses increase, low accumulative rainfall amount, and/or spatial temporal variation of rainfall are large. In the case of simulated sediment concentrations, the

differences are higher than simulated water discharges, variation depending on the catchment size and characteristics as well as.

The analyses spatial scale dependency of a lumped sediment runoff model derived from a physically-based distributed sediment runoff model under land use and rainfall scenario and it application for large catchments are important areas of further research.

ACKNOWLEDGMENTS

This study was supported by the MEXT Coordination Fund for Promotion of Science and Technology, Japan Science and Technology Agency (PI: Prof. Kaoru Takara, DPRI, Kyoto University).

REFERENCES

Apip., Sayama, T., Tachikawa., Y. and Takara, K. (2008), Lumping of a physically-based distributed model for sediment runoff prediction in a catchment scale, *Annual Journal of Hydraulic Engineering, JSCE*, Vol. 52, pp 43-48.

Apip., Sayama, T., Tachikawa., Y. and Takara, K. (2007), The spatio-temporal predictions of rainfall-sediment-runoff based on lumping of a physically-based distributed model, *Annuals of Disas*. Prev. Res. Inst., Kyoto Univ., No. 50B, pp. 79-94.

Ichikawa, Y., Oguro, T., Tachikawa, Y., Shiiba, M., and Takara, K. (2000), Lumping general kinematic wave equation of slope runoff system (in Japanese), *Annual Journal of Hydraulic Engineering, JSCE*, 44, pp. 145-150, 2000.

Sivapalan, M., C. (2002), Linearity and non-linearity of basin response as a function of scale: Discussion of alternative definitions, *Water Reour. Res.,* Vol. 38(2), 1012, doi:10.1029/2001WR000482.

Takara, K., Nakayama, D., Tachikawa, Y., Sayama, T., Nakagawa, H., Satofuka, Y., Egashira, S., and Fujita, M. (2007), A Rainfall-Sediment-Runoff model in the Upper Brantas River, East Java, Indonesia. *Annuals of Disas. Prev. Res. Inst., Kyoto Univ.*, No. 44 B-2, 2007.

Takara, K., Yamashita, T., Egashira, S., Dyah, P.R., Irwan, S., Syamsudin, A.R., and Anton. (1996), Application of Remote Sensing and GIS to Research on Disasters Caused by Floods and Sedimentation. In *Proceedings of Workshop on Disasters Caused by Floods and Geomorphological Changes and Their Mitigations (WDFGM-1996);* Dyah, P.R., Raharjanto, Sudarminto, Agus, S., Isnugroho, and Djamal, H. (Ed.), pp. 62-77.

Yang, C. T. (1973), Incipent motion and sediment transport. *J. Hydraul. Div. Am. Soc. Civ. Eng*., Vol. 99, No. HY10, pp. 1679-1704.

Yang, C. T. (1979), Theory the minimum rate of energy dissipation. *J. Hydraul. Div. Am. Soc. Civ. Eng*., Vol. 105, No. HY7, pp. 1679-1704.

TECHNICAL CONTRIBUTIONS

Turbulent Flow Structure